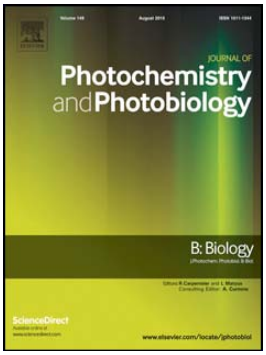

New palladium(II) hydrazone complexes: Synthesis, structure and biological evaluation

Ganesan Ayyannan, Maruthachalam Mohanraj, Gunasekaran Raja, Nanjan Bhuvanesh, Raju Nandhakumar, Chinnasamy Jayabalakrishnan

PII: S1011-1344(16)30502-4
DOI: doi: 10.1016/j.jphotobiol.2016.08.003
Reference: JPB 10508

To appear in:

Received date: 29 June 2016
Revised date: 1 August 2016
Accepted date: 1 August 2016

Please cite this article as: Ganesan Ayyannan, Maruthachalam Mohanraj, Gunasekaran Raja, Nanjan Bhuvanesh, Raju Nandhakumar, Chinnasamy Jayabalakrishnan, New palladium(II) hydrazone complexes: Synthesis, structure and biological evaluation, (2016), doi: 10.1016/j.jphotobiol.2016.08.003

New palladium(II) hydrazone complexes: Synthesis, structure and biological evaluation

Ganesan Ayyannan[a], Maruthachalam Mohanraj[a], Gunasekaran Raja[a], Nanjan Bhuvanesh[b], Raju Nandhakumar[b], Chinnasamy Jayabalakrishnan[a]*

[a]*Post-Graduate and Research Department of Chemistry, Sri Ramakrishna Mission Vidyalaya College of Arts and Science, Coimbatore - 641 020, Tamil Nadu, India.*
[b]*Department of Chemistry, Karunya University, Karunya nagar, Coimbatore - 641 114, Tamil Nadu, India.*

*Corresponding author contact details, e-mail address: drcjbstar@gmail.com (C.Jayabalakrishnan), Tel.: +0422 2692461, Fax: 0422 2693812.

Abstract

Two new palladium(II) complexes of 4-hydoxy-benzoic acid (5-bromo-2-hydroxy-benzylidene)-hydrazide (H_2L) (**1**) with triphenylphosphine and triphenylarsine as coligand have been synthesized and characterized by the aid of various spectral techniques. The structure of the ligand and complexes was confirmed by single crystal X-ray diffraction studies. The hydrazone ligand acts as a tridendate ligand with ONO as the donor sites and is preferably found in the enol form in all the complexes. The structural analysis of **2** and **3** confirms the square planar geometry of the two complexes. The DNA binding of these complexes and ligand calf thymus DNA (CT-DNA) was investigated by using various methods, which revealed that the compounds interacted with CT-DNA through intercalation. Binding properties of the free ligand and its complexes with bovine serum albumin (BSA) protein have been investigated using UV-visible and fluorescence spectroscopic methods which indicated the stronger binding nature of the palladium complexes to BSA than the free hydrazone ligand. In addition, concentration dependent free radical scavenging potential of all the synthesised compounds (**1-3**) was also carried out under *in vitro* conditions. Further, the *in vitro* cytotoxicity of the compounds was examined on a HeLa and MCF-7 cell lines, which revealed that complex **2** exhibited a superior cytotoxicity than complex **3** and ligand **1**.

Keywords:
Palladium(II) complexes; Nucleotide and protein interaction; Antioxidant; Cytotoxicity.

Introduction

In recent years, design and synthesis of transition metal complexes and to find the interaction ability with DNA and protein is an interest field of medicinal chemistry. Due to metal complexes binding to DNA or protein, are commonly considered as the main molecular targets in the action of basis of designing and discovering new and more efficient anticancer drugs [1-5]. Cisplatin is widely used and well-known metal based drug for cancer therapy, represents a major landmark in the history of metal-based anticancer drugs. However, the clinical success of cisplatin is limited by significant side effects that originate from its binding mode with DNA and the formation of covalent cross-links [6-8]. Therefore, much attention has been paid to the design and synthesis of new metal-based drugs bearing metal ions other than platinum with more-efficacious, target-specific, less-toxic and non-covalent DNA-binding [9, 10]. Small molecules of drug can interact with DNA through the following three non-covalent modes: intercalation, groove binding and external static electronic effects. Intercalation is one of the most important DNA binding modes because it invariably leads to cellular degradation. The planarity, coordination geometry, and type of donor atom present in ligand play key roles in determining the intercalating ability of metal complexes with DNA [11]. The metal ion type and its valence, which are responsible for the geometry of the complexes, also influence the intercalating ability of metal complexes. In this regard, the square-planar geometry of the palladium complexes showed a remarkable intercalation binding properties with DNA.

Based on the aspect of the metallic ion, because of the similar coordination modes and chemical properties of palladium(II) and platinum(II), they both form square planer complexes. On the basis of the structural and thermodynamic analogy between platinum(II) and palladium(II) complexes, much attention has been paid to palladium(II) compounds as potential anticancer agents [12]. Palladium(II) complexes undergo aquation and ligand exchange reactions 10^5 times faster than the corresponding platinum(II) complexes [13]. Furthermore, number of mixed ligand palladium(II) complexes are tested and proved to be an efficient compounds of antitumor drugs [14-19]. In addition, hydrazones are important class of ligands with interesting ligation properties due to the presence of several coordination sites and are widely applied in the field of insecticides, medicines and analytical reagents due to their excellent bioactivity [20-24]. The formation of palladium complexes with hydrazone ligand plays an important role to enhance their biological activity.

On the other hand, binding of drugs with proteins have also attracted enormous research interest as a prime molecular target [25]. The magnitude of the albumin interactions with the drug is essential since it plays a dominant role in drug disposition and efficacy. The bound drug can act as a depot while the unbound drug produces the desired pharmacological effect. Therefore, the interactions with proteins play an important role in the absorption, transportation and deposition of a variety of endogenous and exogenous substances such as fatty acids drugs and metal ions in blood stream [26]. Therefore interaction studies of the metal complexes with biomolecules like DNA and BSA become very important to develop new drugs with great potential. In this respect, we have synthesis and characterization of two new palladium(II) hydrazone complexes [Pd(PPh_3)L] (**2**) and [Pd($AsPh_3$)L] (**3**). The molecular structure of palladium(II) complexes are determined by single crystal X-ray diffraction method. Further, a series of experiments have been carried out to study the interaction of palladium(II) complexes and free ligand with nucleic acid and BSA. Also, *in vitro* free radical scavenging and cytotoxic activities has also been carried out.

Experimental section

Materials and methods

All the reagents used were of analytical or chemically pure grade. Solvents were purified and dried according to standard procedures [27]. Doubly distilled water was used to prepare buffers. Ethidium bromide (EB), bovine serum albumin (BSA), calf thymus DNA (CT-DNA) were purchased from Sigma-Aldrich and used as received. The ligand and the starting complexes [$PdCl_2(PPh_3)_2$] [$PdCl_2(AsPh_3)_2$] were prepared according to the previous report [28, 29]. Microanalyses (C, H and N) were performed on a Vario EL III CHNS analyser. IR spectra were recorded as KBr pellets in the 400-4000 cm^{-1} region using a Perkin Elmer FT-IR 8000 spectrophotometer. Electronic spectra were recorded in DMSO solution with a Systronics double beam UV-vis spectrophotometer 2202 in the range 200-800 nm. Fluorescence spectral data were performed on a JASCO FP-8200 fluorescence spectrophotometer at room temperature. ^{1}H, ^{13}C and ^{31}P NMR spectra were recorded on a Bruker AV III 500 MHZ instrument using TMS and ortho phosphoric acid as an internal standard. Melting points were recorded with Veego VMP-DS heating table.

Synthesis of hydrazone ligand (H_2L) (1)

The ligand, 4-hydoxy-benzoic acid (5-bromo-2-hydroxy-benzylidene)-hydrazide (H_2L) (**1**) was prepared by refluxing an equimolar mixture of 4-hydroxy benzoic acid hydrazide (0.152

g; 1 mmole) and 5-bromo-2-hydroxy benzaldehyde (0.201g; 1 mmole) in 50 ml methanol for 6 h (Scheme 1). The reaction mixture was cooled to room temperature and the solid obtained was filtered, washed several times and recrystallized from methanol. White coloured crystals suitable for X-ray diffraction analysis were obtained by slow evaporation of its methanolic solution**.** Yield: 84%; Melting point: 259°C. Elemental Analysis: Found (calculated) (%) $C_{14}H_{11}BrN_2O_3$: C, 51.93 (50.17); H, 3.11 (3.31); N, 8.18 (8.36). IR (KBr, cm^{-1}): 3302 ν(NH); 1610 ν(C=O); 1599 ν(C=N); 1103 ν(N-N); UV-vis (DMSO), λ_{max} (nm) (ε M^{-1} cm^{-1}): 304 (6240), 358 (3925) ($\pi \rightarrow \pi^*$, $n \rightarrow \pi^*$). ^{1}H NMR (DMSO-d_6): δ 12.01 (s, 1H, hydrazine NH), δ 8.58 (s, 1H, H-C=N), δ 11.42 (s, 1H, o-OH), δ 10.19 (s, 1H, p-OH), δ 7.84 (d, 1H, aromatic CH), δ 7.77 (d, 1H, aromatic CH), δ 7.43 (d, 1H, aromatic CH), δ 7.41 (d, 2H, aromatic CH), δ 6.9 (d, 2H, aromatic). ^{13}C NMR: δ 163 (C=O), δ 161 (C=N), δ 110.44, 115.21, 118.68, 121.31, 123.16, 129.90, 130.80, 133.35, 134.40, 145.29 (aromatic).

Synthesis of [Pd(L_2)(PPh_3)] (2)

To a warm methanolic solution (25 ml) of H_2L (0.0335g; 0.1 mmole), dichloromethane solution of [$PdCl_2(PPh_3)_2$] (0.0701 g, 0.1 mmole) was added and followed by two drops of triethylamine. The reaction mixture was refluxed 1 h and kept at room temperature for crystallization. Needle like orange red crystals suitable for X-ray studies were obtained on slow evaporation. Yield: 79%, Melting point: 221°C. Elemental Analysis: Found (calculated) (%) $C_{32}H_{24}BrN_2O_3PPd$: C, 52.56 (54.76); H, 3.76 (3.45); N, 3.90 (3.99). Selected IR bands (cm^{-1}): 1590 ν(C=N); 1353 ν(enolic C-O); 1423, 1095, 690 (for PPh_3). UV-vis (DMSO), λ_{max} (nm) (ε M^{-1} cm^{-1}): 302 (9170), 368 (8221) (intra-ligand transitions); 409 (7253), 424 (6560) (LMCT). ^{1}H NMR (DMSO-d_6): δ 8.53 (s, 1H, H–C=N), δ 9.93 (s, 1H, p-OH), δ 7.70 (d, 1H, aromatic CH), δ 7.68 (d, 1H, aromatic CH), δ 7.66 (d, 1H, aromatic CH), δ 7.65 (d, 2H, aromatic CH), δ 7.63 (d, 2H, aromatic CH), δ 7.32 (d, 6H, aromatic CH), δ 6.75 (d, 6H, aromatic CH), δ 6.64 (d, 3H, aromatic CH), ^{13}C NMR: δ 158 (C-O), δ 171 (C=N), δ 144.61, 134.65, 134.55, 133.21, 132.31, 131.16, 130.78, 130.61, 128.78, 128.31, 127.31, 126.22, 118.89, 114.21 (aromatic). ^{31}P NMR: δ 20.8.

Synthesis of [Pd(L_1)($AsPh_3$)] (3)

It was prepared as described for **2** by the reaction of [$PdCl_2(AsPh_3)_2$] (0.0789 g, 0.1 mmole) with ligand (0.0290g; 0.1 mmole). Dark orange coloured crystals obtained were found to be suitable for X-ray diffraction. $C_{32}H_{24}BrN_2O_3AsPd$ (**3**): Yield: 81%, MP: 280 °C. Anal. calcd. (%): C, 51.53; H, 3.45; N, 3.24. Found (%): C, 50.68; H, 3.37; N, 4.13. Selected IR bands (cm^{-1}): 1593 ν(C=N); 1356 ν(enolic C-O); 1423, 1084, 693 (for $AsPh_3$). UV-vis (DMSO),

λ_{max} (nm) (ε M^{-1} cm^{-1}): 305 (7673), 368 (7111) (intra-ligand transitions); 406 (5995), 432 (5880) (LMCT). ^{1}H NMR (DMSO-d_6): δ 8.52 (s, 1H, H–C=N), δ 9.97 (s, 1H, p-OH), δ 7.71 (d, 1H, aromatic CH), δ 7.65 (d, 1H, aromatic CH), δ 7.59 (d, 1H, aromatic CH), δ 7.37 (d, 2H, aromatic CH), δ 7.36 (d, 2H, aromatic CH), δ 7.31 (d, 6H, aromatic CH), δ 6.76 (d, 6H, aromatic CH), δ 6.70 (d, 3H, aromatic CH), ^{13}C NMR: δ 159 (C-O), δ 173 (C=N), δ 144.84, 135.13, 134.95, 133.32, 132.72, 131.69, 130.93, 130.11, 129.42, 128.89, 121.19, 115.11, 109.12, 105.87 (aromatic).

Single crystal X-ray diffraction studies

Single crystal X-ray diffraction data of **1**, **2** and **3** were collected at room temperature on a Bruker AXS KAPPA APEX2 CCD diffractometer equipped with a fine focused sealed tube. The unit cell parameters were determined and the data collections of **1**, **2** and **3** were performed using a graphite-mono chromate Mo Kα(k = 0.71073 Å) radiation by u and x scans. The data collected were reduced SAINT program [30] and the empirical absorption corrections were carried out using the SADABS program [31]. The structure of the ligand and complexes was solved by direct methods [32] using SHELXS-97, which revealed the position of all non-hydrogen atoms, and was refined by full-matrix least squares on F^2 (SHELXL- 97) [33]. All non-hydrogen atoms were refined anisotropically, while the hydrogen atoms were placed in calculated positions and refined as riding atoms.

DNA binding experiments

Absorption titration

In order to identify the binding mode of the synthesized compounds (**1-3**) with CT-DNA, the UV-visible titration method is used. In absorption titration experiments, the test compounds with CT-DNA were carried out in double distilled water with aminomethane (Tris, 5 mmole) and sodium chloride (50 mmole) (pH = 7.2). The UV absorbance at 260 nm and 280 nm of the CT-DNA solution gave a ratio of 1.8-1.9, indicating that the DNA was sufficiently free of protein [34, 35]. The molar absorption coefficient, ε_{260}, was taken as 6600 $M^{-1}cm^{-1}$. A stock solution of CT-DNA was stored at 277 K and used after no more than 4 days. Absorption titration experiments were performed with a fixed concentration of the compounds (25 μM) while gradually increasing the concentration of DNA (0-50 μM). The blank Tris-HCl buffer (2.5 ml) solution and the compounds (25 μM) were placed in two cuvettes, respectively. To eliminate the absorbance of DNA, an equal amount of DNA was added to both the test solution and the reference solution. After each addition of DNA to the test compounds, the

readings were noted. The magnitude of the binding strength of the test compounds with CT-DNA can be estimated through the binding constant (K_b), which can be obtained by monitoring the changes in the absorbance of the corresponding absorption maxima (λ_{max}) with increasing concentrations of CT-DNA and is given by the equation.

$$[DNA]/[\varepsilon_a - \varepsilon_f] = [DNA]/[\varepsilon_a - \varepsilon_f] + 1/K_b\,[\varepsilon_b - \varepsilon_f]$$

where [DNA] is the concentration of DNA in base pairs, ε_a is the extinction coefficient observed at a given DNA concentration, ε_f is the extinction coefficient of the free complex in solution and ε_b is the extinction coefficient of the complex when fully bound to DNA. In plots of $[DNA]/(\varepsilon_a-\varepsilon_f)$ *versus* [DNA], K_b is given by the ratio of slope to the intercept.

Competitive binding experiments

The competitive DNA binding studies of the new synthesized compounds (**1**-**3**) with ethidium bromide (EB) was investigated with fluorescence spectroscopy in order to inspect whether the compound could displace bound EB from the DNA-EB complex by the addition of the solution of the respective compounds (**1**-**3**) to the Tris-HCl buffer of the DNA-EB mixture. Before measurements were taken, the mixture was shaken up and recorded. The fluorescence spectra of DNA bound EB were obtained in the excitation (λ_{ex}) and emission (λ_{em}) wavelengths of 515 and 602 nm, respectively. Before measurements, the system was shaken and incubated at room temperature for 5 min. The emission was recorded at 530-750 nm. The quenching constants of compounds (**1**-**3**) were evaluated qualitatively by employing Stern-Volmer equation [36],

$$F_0 / F = K_q / [Q] + 1$$

where F_0 is the emission intensity in the absence of complex, F is the emission intensity in the presence of complex, K_q is the quenching constant, and [Q] is the concentration of the compound. The K_q value has been obtained as a slope from the plot of F_0 / F versus [Q]. Further, the binding constant (K_{app}) value obtained for the compounds using the following equation.

$$K_{EB}[EB] = K_{app}[compound]$$

where the compound concentration is the value at a 50% reduction in the fluorescence intensity of EB, K_{EB} ($1.0 \times 10^7 M^{-1}$) is the DNA binding constant of EB, [EB] is the concentration of EB = 10 μM.

Cyclic voltammetry assay

Voltammetric techniques are complementary to other related biophysical techniques that are applied to study the interaction between the redox active molecules and biomolecules. This electrochemical study were performed on a CHI 604A electrochemical analyzer with three electrode system of glassy carbon as the working electrode, a platinum wire as auxiliary electrode and Ag/AgCl as the reference electrode. Solutions were deoxygenated by purging with N_2 prior to measurements. The supporting electrolyte was used 50 mmole NaCl and 5 mmole Tris-HCl buffer at pH 7.2. In order to determine diffusion coefficients before and after the addition of DNA with palladium(II) complexes, voltammetric responses were recorded at various scan rates.

Viscosity measurements

The viscosity of a DNA solution has been measured in the presence of increasing amounts of synthesized compounds. Flow time was measured with a digital stop watch three times for each sample and an average flow time was calculated. The relative viscosities for DNA in the absence (η_o) and presence (η) of the compounds was calculated using the relation $\eta = (t\text{-}t_o)/t_o$, where t and t_o are the observed flow time for each sample and buffer [37]. The values of relative viscosity $(\eta/\eta_o)^{1/3}$ were plotted against R, where R= [DNA]/[compound].

Protein binding studies

The binding of synthesized compounds with bovine serum albumin (BSA) were studied using fluorescence spectra recorded at affixed excitation wavelength corresponding to bovine serum albumin (BSA) as 280 nm and monitoring the emission at 345 nm. The excitation and emission slit widths and scan rates were constantly maintained for all the experiments. Samples were carefully degassed using pure nitrogen gas for 15 min by using quartz cells (4 × 1 × 1 cm) with high vacuum Teflon stopcocks. Stock solution of BSA was prepared in 50 mM tris-HCl buffer (pH = 7.2) and stored in the dark at 4ºC for further use. Concentrated stock solutions of ligand and complexes were prepared by dissolving them in DMSO: tris-HCl buffer (1:100) and diluted suitably with buffer to required concentrations. 2.5 ml of BSA solution (1 µM) was titrated by successive additions of a 25 ml stock solution of compounds (0-25 µM) using a micropipette.

Antioxidant assays

The 2,2-diphenyl-1-picrylhydrazyl (DPPH) radical scavenging activity of the synthesized compounds was measured according to the method of Blois [38]. The DPPH radical is a

stable free radical having a λ_{max} at 517 nm. A fixed concentration of the experimental compounds was added to a solution of DPPH in methanol (125 µM, 2 mL), and the final volume was made up to 4 mL with double distilled water. The solution was incubated at 37 ºC for 30 min in the dark. The decrease in absorbance of DPPH was measured at 517 nm.

The hydroxyl (OH) radical scavenging activities of the complexes have been investigated using the Nash method [39]. *In vitro* hydroxyl radicals were generated by Fe^{3+}/ascorbic acid system. The detection of hydroxyl radicals was carried out by measuring the amount of formaldehyde formed from the oxidation reaction with DMSO. The formaldehyde produced was detected spectrophotometrically at 412 nm. A mixture of 1.0 mL of iron-EDTA solution (0.13% ferrous ammonium sulphate and 0.26% EDTA), 0.5 mL of EDTA solution (0.018%), and 1.0 mL of DMSO (0.85% DMSO (v/v) in 0.1 M phosphate buffer, pH 7.4) were sequentially added in the test tubes. The reaction was initiated by adding 0.5 mL of ascorbic acid (0.22 %) and incubated at 80-90 ºC for 15 min on a water bath. After incubation, the reaction was terminated by the addition of 1.0 mL of ice-cold TCA (17.5% w/v). Subsequently, 3.0 mL of Nash reagent was added to each tube and left at room temperature for 15 min. The intensity of the colour formed was measured spectrophotometrically at 412 nm against a reagent blank.

Assay of nitric oxide scavenging activity is based on the Green method [40], where sodium nitroprusside in aqueous solution at physiological pH spontaneously generates nitric oxide, which interacts with oxygen to produce nitrite ions that can be estimated using Greiss reagent. Scavengers of nitric oxide compete with oxygen leading to reduced production of nitrite ions. For the experiment, sodium nitroprusside (10 mmole) in phosphate buffered saline was mixed with a fixed concentration of the compound and incubated at room temperature for 150 min. After the incubation period, 0.5 mL of Griess reagent containing 1% sulfanilamide, 2% H_3PO_4 and 0.1% N-(1-naphthyl) ethylenediamine dihydrochloride were added. The absorbance of the chromophore formed was measured at 546 nm.

For each of the above assay, tests were done in triplicate by varying the concentration of the complexes ranging from 10-50 µM. The percentage activity was calculated by using the formula, % activity = $[(A_0–A_c)/A_0] \times 100$, where A_0 and A_c represent the absorbance in the absence and presence of the test compounds, respectively. The 50% activities (IC_{50}) were calculated from the results of percentage activity.

Evaluation of cytotoxicity

Cytotoxicity of the ligand and palladium complexes was evaluated on human cervical (HeLa) and human breast (MCF-7) cell lines. Cell viability was carried out using the 3-[4, 5-dimethylthiazol-2-yl] 2, 5-diphenyltetrazolium bromide (MTT) assay method [41]. The MCF-7 and HeLa cells were grown in Eagles minimum essential medium containing 10% fetal bovine serum (FBS). For screening experiment, the cells were seeded into 96-well plates in 100 mL of respective medium. The test compounds (**1**-**3**) dissolved in DMSO was seeded to the wells. Triplication was maintained, and the medium without the compounds served as the control. After 24 h, the wells were treated with 20 µL MTT [5 mg mL^{-1} phosphate buffered saline (PBS)] and incubated at 37 °C for 4 h. The medium with MTT was then removed separately and the formed formazan crystals were dissolved in 100 mL DMSO. The absorbance was then measured at 570 nm using micro plate reader. The % cell inhibition was determined using the following formula, % cell inhibition=100-Abs (sample)/Abs (control) × 100. The IC_{50} values were determined from the graph plotted between % cell inhibition and concentration.

RESULTS & DISCUSSION

Synthesis

The stoichiometric reactions of $[PdCl_2(EPh_3)_2]$ (where E = P or As) with hydrazone ligand (H_2L) in 1:1 methanol/dichloromethane resulted in the formation of new complexes $[Pd(PPh_3)L]$ (**2**) and $[Pd(AsPh_3)L]$ (**3**) (Scheme 2), where the hydrazone ligand acted as a tridentate ONO ligand. The analytical data confirms the stoichiometry of the complexes. The structures of the ligand (**1**) and complexes (**2** and **3**) were confirmed by the X-ray crystallographic study. All of the three synthesized compounds are quite stable in air, light and soluble in most of the organic solvents, such as methanol, ethanol, CH_2Cl_2, $CHCl_3$, DMF and DMSO.

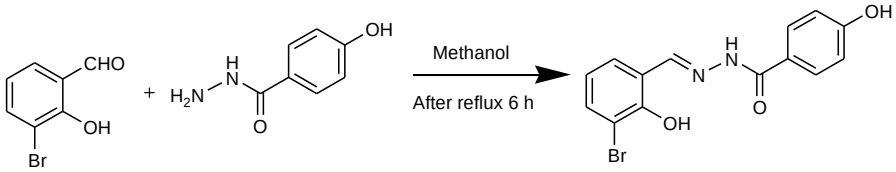

Scheme 1. Synthesis of hydrazone ligand.

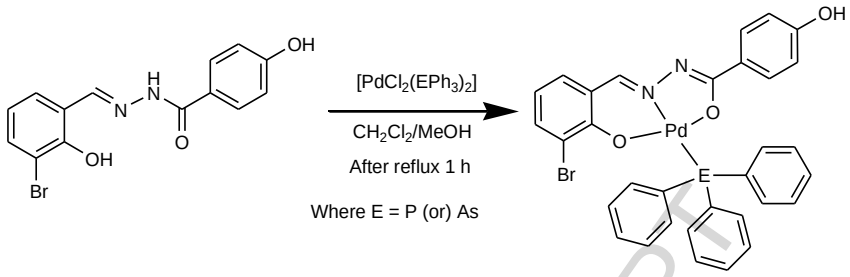

Scheme 2. Synthesis of the palladium(II) complexes

Spectroscopic studies

The electronic spectra of ligand and Palladium(II) complexes have been recorded in DMSO solvent and they displayed two to three bands in the region around 302-432 nm. Electronic spectra of **1** showed two strong absorption bands at 304 and 358 nm, which are assigned to π-π* and n-π* transitions respectively. In the electronic spectra of the complexes, the bands appeared in the region 302-368 nm have been assigned to intra ligand transition [42] and the bands around 406-432 nm have been assigned to metal to ligand charge transfer transition [43].

The infrared spectra of the palladium(II) complexes (**2** and **3**) compared with that of the free ligand (H_2L) provide significant information regarding to the coordination mode of ligand in new metal complexes. The IR spectra of the ligand showed a strong absorption at 1599 cm^{-1} due to the presence of azomethine group. In complexes this has been shifted to lower frequency (1590 and 1593 cm^{-1}) indicating the coordination of azomethine nitrogen to palladium [44]. The (C=O) and (N-H) bands appeared at 1660 and 3302 cm^{-1} respectively in the free ligand completely disappeared in the complexes and a new band (C-O) appeared at 1353 and 1356 cm^{-1} for the complexes (**2**) and (**3**) respectively, which indicating the enolisation of NH-C=O group and subsequent coordination through the deprotonated oxygen atom [45]. In addition, the bands confirming the presence of triphenyl phosphine and arsine in were observed in the expected region [46]. All these facts suggested that the ligand H_2L were coordinated to palladium(II) ion *via* the phenolate oxygen, the azomethine nitrogen and the imidolate oxygen in complexes.

The ^1H NMR spectra of the ligand H_2L and the corresponding palladium(II) complexes were recorded in DMSO-d_6 solvent. In the spectra of H_2L, a sharp singlet corresponding to the phenolic -OH group has appeared at 11.42 ppm. However, this singlet completely disappeared in the two complexes confirmed the involvement of phenolic oxygen in coordination with Pd(II) ion. Also, a weak singlet appeared at 12.01 ppm has been

assigned to the NH proton. In the spectrum of the complexes (**2** and **3**) there was no such resonance attributable to NH, which indicates the coordination of the enolate oxygen atom after enolisation and subsequent deprotonation [47]. The spectrum of H_2L showed a sharp singlet at 8.58 ppm corresponding to azomethine proton. However, in case of the complexes (**2** and **3**), the singlet at 8.58 ppm gets shifted (for **2** and **3** are 8.53 and 8.52 ppm, respectively) due to the coordination of azomethine N with Pd(II) ion. The spectra of **1**, **2** and **3** show multiplets at 6.58-7.89 ppm due to the presence of aromatic protons [48].

The ^{13}C NMR spectra of the ligand, displayed well defined signal at δ 163 corresponding to the carbonyl carbon (C=O), which disappears in the spectra of the complexes and appears as a new signal at 159 and 158 ppm (C-O) indicating the coordination of oxygen *via* deprotonation. The spectra of the ligand show a single resonance at 161 ppm due to the azomethine carbon atom, the downfield shift of the complexes signal at 171 and 173 ppm clearly indicates the coordination of C=N [49]. The aromatic carbons of the free ligand and complexes show signal in the regions 105-147 ppm [50].

In addition, to confirm the presence of triphenylphosphine group, ^{31}P NMR spectra were recorded for the complex **2**. A sharp singlet observed at 20.8 ppm for the complex **2** was due to the presence of phosphorous atom and thus suggesting the presence of triphenylphosphine group in complex **2** [51].

Based on IR, UV-vis, ^{1}H, ^{13}C and ^{31}P NMR data, the hydrazone ligand is coordinated to the palladium ion by square planar geometry in a tridentate fashion by replacing both chloride ions and the triphenylphosphine/triphenylarsine from the starting precursors. Further the geometry of the complexes confirmed by X-ray diffraction studies.

X-ray crystallography

Needle shaped crystals suitable for X-ray diffraction studies were grown from a solution of H_2L in methanol. The summary of the data collected and the refinement parameters are given in Table 1. The selected bond lengths and bond angles are given in Table 2. An ORTEP representation of **1** is shown in Figure 1. The crystals of hydrazone ligand **1** in the orthorhombic space group P*na*2_1 and unit cell comprises of four molecules. The azomethine C(7)-N(1) bond length, 1.278(4) Å is in conformity with a formed C=N double bond length, 1.28 Å. The bond distances in the hydrazone side chain agree well with the values observed for other hydrazones where the C(8)-O(2) group is present in the keto form 1.229(3) Å. And the bond distances for N(1)-N(2) at 1.378(3), and for C(8)-N(2) at 1.354(4) Å are closer to N-

N and N-C normal single bonds respectively. The oxygen O(2) atom and the hydrazine nitrogen N(1) are in a *trans* position with respect to the C(8)-N(2) bond 1.354(4) Å.

The mononuclear structure of the newly synthesized palladium(II) complexes **2** and **3** are determined by single crystal X-ray diffraction in order to identify the exact coordination mode of hydrazone ligand in the complexes (Fig. 2 and 3). The selected bond lengths and bond angles are summarised in Table 3. The single crystal X-ray study reveals that the complexes **2** and **3** crystallized in monoclinic space group $P2_1/c$ with four molecules per unit cell. In the complexes (**2** and **3**), the Pd(II) ion is coordinated to the dibasic tridentate ligand through enolate oxygen (Pd-O bond distances of 1.9961(19) A˚ and 1.993(2) A˚ respectively), phenolic oxygen (Pd-O bond distances of 1.9625(19) A˚ and 1.958(2) A˚ respectively) and the nitrogen atom (Pd-N bond distances of 1.981(2) A˚ and 1.970(3) A˚ respectively). The remaining coordination site is occupied by triphenylphosphine and triphenylarsine satisfying the fourth coordination site in **2** and **3** respectively. In complexes, the Pd–P and Pd–As bond lengths of 2.2864(8) and 2.3920(5) Å for **2** and **3** respectively are close to the reported value of palladium(II) complexes [53]. The triphenylphosphine and triphenylarsine in the complexes N(1) nitrogen are mutually *trans* to each other. The trans angles are N(1)-Pd(1)-P(1), 171.44(6)°, and O(3)-Pd(1)-O(1), 172.74(8)° (for **2**), N(1)-Pd(1)-As(1), 171.14(8)°, and O(3)-Pd(1)-O(1), 172.74(8)°(for **3**) which deviate considerably from the ideal angle of 180°, suggesting distortion in the square planar coordination geometry of the complexes. The C=O bond distance in C(8)-O(2) of the free ligand is found to be 1.229(3) Å. Whereas, upon complexation, the value of C(1)-O(1); 1.308(3) Å for **2** and C(7)-O(1); 1.303(4) Å for **3** due to the enolization of oxygen. There is an increase in the C=N bond lengths C(8)-N(1); 1.278(4) Å for **2** and 1.285(4) Å for **3** compared to ligand 1 C(7)-N(1); 1.278(3) Å due to azomethine nitrogen involved in coordination. The selected bond lengths and bond angles agree very well with those that are reported for other palladium(II) complexes [54].

Nucleic acid binding studies

Electronic absorption titration

Electronic absorption spectroscopy is employed to determine the binding mode of test compounds with DNA. The absorption spectra of compounds (**1**-**3**) were recorded with a fixed concentration of the compounds in the absence and presence of different concentrations of CT-DNA and the results are shown in Fig. 4. The absorption spectra of ligand (**1**) mainly consist of two resolved bands [Intra ligand transitions (IL)] centered at 291 and 355 nm. As

the DNA concentration is increased, the bands at 291 and 355 nm showed 18.32% and 12.91% hypochromism, respectively without any shift in the absorption maxima. For complex **2**, upon addition of DNA, the intra ligand band at 265 and 323 nm exhibited hypochromism of 61.39% and 60.12% with a red shift of 1 and 4 nm respectively. The CT band at 413 nm showed 63.53% hypochromism with a red shift of 3nm in the absorption maxima. Similarly, complex **3** exhibited hypochromism (IL) at 281 (25.59%) and 328 nm (66.89%) with a red shift of 3 and 4 nm, respectively. In addition, complex **3** showed hypochromism (CT) at 409 nm (22.31%). Generally, a compound binding to DNA through intercalation mode results in hypochromism with or without a small red or blue shift, due to a strong stacking interaction between the planar aromatic chromophore of the compound and the base pairs of DNA [55, 56]. These results revealed that the compounds **1**, **2** and **3** with bind to the DNA helix *via* intercalation. After the compounds intercalate to the base pairs of DNA, the π^* orbital of the intercalated compounds could couple with π orbital of the base pairs, thus decreasing the $\pi \rightarrow \pi^*$ transition energies, resulted hypochromism. The complexes, **2** and **3** showed more hypochromicity with red shift than the ligand (H_2L), indicating that the binding strength of the palladium(II) complexes is much stronger than that of the free ligand.

The magnitudes of the intrinsic binding constants (K_b) were calculated to be $9.96 \times 10^3 M^{-1}$ for the ligand (H_2L) and $6.78 \times 10^4 M^{-1}$ and $2.04 \times 10^4 M^{-1}$ for complexes **2** and **3**, respectively (Fig. 5 and Table 4). The observed values of K_b revealed that the ligand and the palladium(II) complexes bind to DNA *via* an intercalative mode. These results are similar with the earlier reported for the intercalative mode of various metallointercalators [57]. From the above results obtained, it has been found that both the palladium complexes (**2** and **3**) exhibit a good binding affinity to DNA, greater than that of the corresponding free ligand. This is mainly due to the chelation of the palladium metal with the ligand. It has been found that complex **2** strongly bound with CT-DNA relative to that with **1** and **3**, and the order of binding affinity is **2**>**3**>**1**. The different DNA-binding properties of the palladium complexes **2** and **3** are due to the two different co-ligands present.

Ethidium bromide displacement assay

The competitive DNA binding of compounds has been studied by monitoring changes in emission intensity of ethidium bromide (EtBr) bound to CT-DNA by the addition of compound concentration (**1-3)** as quenchers. The fluorescence emission intensity of EB can be quenched by the addition second DNA binding molecule by either replacing the DNA bound EB or accepting an excited-state electron from EB. Fig. 6 shows the fluorescence

spectra of DNA-bound EB by compounds and as the concentration of the compounds increases, the emission band at 613 nm exhibited hypochromism up to 14.88, 20.20 and 21.11% with blue shifts of 3, 2, and 3 nm of the initial fluorescence intensity for **1**-**3** respectively. This indicates that both the complexes and the free ligand could compete with EB in binding to DNA and complex **2** binds to DNA stronger than other **1** and **3**. From the results observed, decrease in the fluorescence intensity clearly indicates that the EB molecules are displaced from their DNA binding sites and are replaced by the complexes under investigation [58].

Further, the analysis of the quenching data using Stern-Volmer equation gave the corresponding K_q values and the apparent binding constant (K_{app}) values (Fig.7 and Table 4). The quenching constant (K_q) values for **1**, **2** and **3** were found to be 2.54×10^4 M^{-1}, 3.66×10^4 M^{-1} and 3.01×10^4 M^{-1}, respectively. Furthermore, the apparent binding constant (K_{app}) values obtained for the corresponding complexes 1 and 2 were found to be 1.8×10^5 M^{-1}, 2.7×10^5 M^{-1} and 2.2×10^5 M^{-1}, respectively. The results suggest that complex **2** intercalated more strongly than complex **3**. The binding activities of the palladium(II) complexes may be better than that of the free hydrazone ligand.

Cyclic voltammetry assay

The electrochemical method to study about binding of transitional metal complexes to DNA is a useful complement to other investigation methods, such as UV-visible and fluorescence spectroscopies. In general, the electrochemical potential of a small molecule will shift positively when it intercalates into DNA double helix, and it will shift to a negative direction in the case of electrostatic interaction with DNA [58, 59]. Cyclic voltammograms (CV) of the palladium(II) complexes in the absence and presence of CT-DNA in tris-HCl buffer solution are shown in Fig. 8. Upon addition of CT-DNA to a complex solution, no new peaks appeared and the current intensity decreased, these results suggesting the existence of an interaction between each complex and CT-DNA. The decrease in current intensity may be attributed to slow diffusion of the palladium(II) complex to the electrode surface. For addition of CT-DNA complex solution, both the cathodic (E_{pc}) and the anodic (E_{pa}) potentials of **2** and **3** exhibit a positive shift, suggesting an intercalative mode of binding between the complexes and CT-DNA base pairs [60].

Viscosity Measurements

Viscosity measurements are sensitive to changes in length of DNA therefore; its measurement upon addition of a compound is often concerned to clarify the interaction mode of a synthesized compound with DNA. Generally, titrations of DNA by classical intercalating compounds would show increased DNA viscosity, as the DNA helix must lengthen when base pairs are separated to host the binding compounds. And also, a partial or non-classical ligand intercalation causes a compaction in the DNA helix and reducing its effective length of DNA and thereby its viscosity decreases. The effects of the ligand (**1**) and complexes (**2** and **3**) on the viscosity of CT-DNA are shown in Fig. 9. On increasing the amounts of compounds, the relative viscosities of CT-DNA solution increase steadily. The increased degree of viscosity, which may depend on its affinity of compounds to DNA, followed the order of **2**>**3**>**1**. These results further proved that the two palladium(II) complexes and free hydrazone can bind to DNA in the mode of intercalation [61].

On the basis of the above discussion of DNA binding studies, we concluded that the free ligand and palladium(II) complexes can bind to CT-DNA in an intercalative mode and Pd(II) complexes bind to CT-DNA more strongly than the free ligand. The positive results of DNA binding studies for the synthesized compounds prompt us to explore their protein BSA-binding activity and *in vitro* anticancer activity.

BSA-binding properties

UV-vis spectroscopy

The quenching process can occur by different mechanisms, which classified as dynamic quenching and static quenching. In a dynamic quenching mechanism, with the addition of a quencher, only the excited state fluorescence molecule is affected, which results in no change in the absorption spectra of BSA. While, in a static quenching, a new compound is formed between BSA and the quencher, therefore, the absorption spectra of BSA would be considerably affected. It appears that the UV absorption peak goes up or down and with or without any shift of wavelength. The absorption spectra of BSA in the absence and presence of compounds (**1-3**) are shown in Fig. 10. The absorption band obtained for the BSA at 278 nm in the presence of compounds showed an increase in the intensity of absorption after the addition of compounds without any shift, reveals quenching of BSA by the compounds are static quenching processes [62].

Fluorescence quenching studies

Fluorescence quenching techniques have been widely used to study the interaction of small molecules with protein molecules. Fluorescence quenching measurement refers to any process that decreases the fluorescence intensity of a fluorophore due to a variety of molecular interactions including excited-state reactions, molecular rearrangements, energy transfer, ground-state complex formation and collision quenching. Changes in molecular environment in the vicinity of fluorophore can be accessed by the changes in fluorescence spectra in the absence and presence of the test compound and hence provide information to the nature of the binding. The interaction of BSA with the ligand and Pd(II) complexes were studied by fluorescence measurement at room temperature. A solution of BSA (1μM) was titrated with various concentrations of the compound (0-25μM). Fluorescence spectra were recorded in the range of 290-450 nm upon excitation at 280 nm. The changes observed on the fluorescence emission spectra of solution of BSA on the addition of increasing amounts of the compounds are given in Fig. 11. Upon the addition of the new compounds to the BSA solution, a significant decrease of the fluorescence intensity of BSA at 345 nm of up to 70, 82 and 76% from the initial fluorescence intensity of BSA accompanied by a bathochromic shift of 4, 2 and 3 nm for the compounds **1-3** respectively have been observed. The observed red shift is mainly due to the fact that the active site in protein is buried in a hydrophobic environment. This result suggested a definite interaction of all of the compounds with the BSA protein [63].

Further, the fluorescence quenching data were analyzed with the Stern-Volmer equation and the Scatchard equation. From the plot of F_o/F versus [Q], the quenching constant (K_q) can be calculated (Fig. 12). It is assumed that the binding of compounds with BSA occurs at equilibrium and the equilibrium binding constant can be analyzed according to the Scatchard equation.

$$\log[\ (F_o - F) / F\ ] = \log K_{bin} + n \log[Q]$$

where K_{bin} is the binding constant of the compound with BSA and n is the number of binding sites. The binding constant (K_{bin}) and the number of binding sites (n) have been calculated from the plot of $\log[(F_o - F)/F]$ versus log[Q] (Fig. 13). The calculated K_q, K_{bin}, and n values are listed in Table 5. The calculated value of binding site n is around 1 for all of the compounds, indicating the existence of just a single binding site in BSA for all of the compounds. The values of K_q and K_{bin} for all of the compounds suggested that the complexes

interact with BSA more strongly than the ligand. Among the two Pd(II) complexes, the complex (**2**) has better interaction with BSA than the complex (**3**).

Antioxidant activity

Newly synthesized ligand and Pd(II) complexes exhibit good DNA and protein binding ability, it was further considered to study their ability to antioxidant properties of the compounds. Hence, we carried out experiments to investigate the free radical scavenging ability of the ligand and Pd(II) hydrazone complexes against standard antioxidant ascorbic acid (Aca) with DPPH, OH and NO radicals. The IC_{50} values indicated that no significant radical scavenging activities were observed for free ligand under the same experimental conditions. From the experimental results, the IC_{50} value of the complexes with DPPH, OH and NO radical assays were found to be comparable radical scavenging activity with respect to standard antioxidant (Aca) (Table 6). The IC_{50} values show that the ligand and Pd(II) complexes exhibit antioxidant activity in the order of **2**>**3**>**1** in all of the experiments. The palladium complexes having higher antioxidant activity when compared to free ligand, which is due to chelation of the organic ligand with the Pd(II) ion and planarity of the complexes plays an important role in determining the antioxidant properties of the compounds [64]. Moreover, from the results obtained for the two Pd(II) complexes, it can be inferred that the difference in the nature of the complex and the co-ligand present in the complexes are likely to induce variations in antioxidant activities. The complex containing triphenylphosphine as a co-ligand showed better activities than the complex containing triphenylarsine.

***In vitro* cytotoxicity**

From the previous biological studies namely, DNA binding, BSA binding and antioxidant studies the positive results obtained of compounds **1**, **2** and **3** encouraged us to test their cytotoxicity against a panel of human cancer cell lines (human cervical cancer cell line (HeLa) and human breast cancer cell line (MCF-7)) by using MTT assay. The IC_{50} values of the free ligand and palladium hydrazone complexes are given in table 7 and fig. 14. These results observed that the ligand did not show any inhibition of the cell growth even up to 100 µM and clearly indicates chelation of the organic ligand with palladium ion is responsible for the observed cytotoxicity properties of the complexes [65]. The observed result indicates that the palladium complexes **2** and **3** possess great selectivity towards HeLa and MCF-7 cells and display potential application in cancer chemotherapy and less toxic drug. The IC_{50} value showed that both the Pd(II) complexes **2** and **3** exhibited excellent

activity against HeLa and MCF-7 cell lines which was lower than that of the well known anticancer drug cisplatin. The observed higher efficiency of the complex **2** is correlated to the nature of the substitution of the co-ligand, triphenylphosphine coordinated to the central palladium ion. This is due to the liphophilic effect of triphenylphosphine, which favours its permeation through the lipid layer of the cell membrane in the complex and could enhance the activity [66, 67]. The enhanced cytotoxic properties of Pd(II) complexes over the ligand, which may be due to an increase in chelation of the ligand with the Pd(II) ion, cationic nature, and enhanced planarity of the complexes [68, 69]. Hence, these complexes are active against the tumor cell lines under *in vitro* conditions, and the results are comparable to those obtained for other palladium(II) complexes [70]. Though the synthesized complexes were active against tumor cell lines under *in vitro* cytotoxicity experiments, the IC_{50} values are comparable with standard drug cisplatin. The findings of the *in vitro* cytotoxic activities confirm the binding of the complexes to DNA/BSA, which consequently leads to cell death.

Conclusion

Reactions of palladium(II) precursors $[PdCl_2(EPh_3)_2]$ (where E = P or As) with 4-hydoxy-benzoic acid (5-bromo-2-hydroxy-benzylidene)-hydrazide (H_2L) yielded a two new $[Pd(EPh_3)L]$ complexes. The molecular structure of the ligand H_2L and complexes were confirmed by single crystal X-ray diffraction studies. The XRD results of complexes confirmed the distorted square planar geometry around the Pd ion through ONO coordination of **1.** The DNA binding properties of free ligand and palladium(II) complexes were evaluated by the UV-Vis spectra, fluorescence spectra, electrochemical and viscosity measurements which suggest their involvement in intercalative DNA interaction with different binding affinities. From the BSA binding studies, the mechanism of quenching of BSA was found to be a static one indicating that the complexes did effectively bind to BSA interaction than the ligand. All the synthesized compounds exhibit excellent antioxidant activities and the activity of complex **2** showed greater IC_{50} values than the other. In addition, the *in vitro* cytotoxicity assay have been conducted with a cancer cell line demonstrated that both the complexes and free ligand are active against the HeLa and MCF-7 cancer cell line. In particular, complex **2** showed more activity than complex **3** and ligand **1**. This significant activity of **2** might be due to the presence of the phosphine ligand, which is supposed to provide a better cytotoxicity by enhancing lipophilicity and consequently permeability through the lipid layer of the cell membrane. The outcome of this study would be helpful to understand the mechanism of

interactions of palladium(II) hydrazone complexes with nucleic acid and serum albumin and also in the development of potential probes for DNA and BSA structure and conformation of new chemotherapeutic agents.

Acknowledgements

One of the authors, G.Raja gratefully acknowledges University Grants Commission (UGC), Hyderabad, India for financial assistance (NO.F MRP-5925/15 (SERO/UGC)).

References

1 E. Wong and C. M. Giandomenico, *Chem. Rev*., 1999, **99**, 2451-2466.

2 T. G. Drummond, M. G. Hill and J. K. Barton, *Nat. Biotechnol*., 2003, **21**, 1192-1199.

3 E. Meggers and Angew. *Chem., Int. Ed*., 2011, **50**, 2442-2448.

4 4 C. G. Hartinger, N. Metzler-Nolte and P. J. Dyson, *Organometallics*, 2012, **31**, 5677-5685.

5 N. P. Barry and P. J. Sadler, *Chem. Commun*., 2013, **49**, 5106-5131.

6 G. Zhu, M. Myint, W. H. Ang, L. Song and S. J. Lippard, *Cancer Res*., 2012, **72**, 790-800.

7 N. J. Wheate, S. Walker, G. E. Craig and R. Oun, *Dalton Trans*., 2010, **39**, 8113-27.

8 D. Wang and S. J. Lippard, *Nat. Rev. Drug Discovery*, 2005, 4, 307-320.

9 K. Zheng, L. Jiang, Y. T. Li, Z. Yong Wu and C. W. Yan, *RSC Adv*., 2015, **5**, 51730-51744.

10 V. Rajendiran, M. Murali, E. Suresh, S. Sinha, K. Somasundaram and M. Palaniandavar, *Dalton Trans*., 2008, **7**, 148-163.

11 K. Zheng, F. Liu, X. M. Xu, Y.T. Li, Z. Y. Wu, and C. W. Yan, *New J. Chem*., 2014, **38**, 2964-78.

12 J. Ruiz, N. Cutillas, C. Vicente, M. D. Villa, G. Lopez, J. Lorenzo, F.X. Aviles, V. Moreno, D. Bautista, *Inorg. Chem*., 2005, **44**, 7365-7376.

13 S. Ray, R. Mohan, J. K. Singh, M. K. Samantaray, M. M. Shaikh, D. Panda and P. Ghosh, *J. Am. Chem. Soc*., 2007,**129**, 15042-15053.

14 H. Daghriri, F. Huq, P. Beale, *Coord. Chem. Rev*., 2004, **248**,119-133.

15 E. Gao, C. Liu, M. Zhu, H. Lin, Q. Wu, L. Liu, *Anti-Cancer Agents Med. Chem*., 2009, **9**, 356-368.

16 A. S. Abu-Surrah and M. Kettunen, *Curr. Med. Chem*., 2006, **13**, 1337-1357.

17 A. C. F. Caires, *Anti-Cancer Agents Med. Chem*., 2007, **7**, 484-491.

18 A. S. Abu-Surrah, H. H. Al-Sadoni and M. Y. Abdalla, *Cancer Ther*., 2008, **6**, 1-10.

19 A. I. Matesanz, C. Hernandez, A. Rodriguez and P. Souza, *J .Inorg. Biochem*. 2011, **105**, 1613-1622.

20 J. H. Tan, Y. J. Lu, Z. S. Huang, L. Q. Gu and J. Y. Wu, *Eur. J. Med. Chem*., 2007, **42**, 1169-1175.

21 K. Karami, Z. M. Lighvan, S. A. Barzani, A. Y. Faal, M. P. Shirani, T. Khayamian, V. Eigner and M. Dusek, *New J. Chem*., 2015, **39**, 8708-8719.

22 N. Miklasova, E. Fischer-Fodor, P. Lonnecke, C. Ionut¸ Tomuleasa, P. Virag , M. P. Schrepler, R. Mikla, Luminit¸ S. Dumitrescu and E. Hey-Hawkins, *Eur. J. Med. Chem*., 2012, **49**, 41-47.

23 K. Karami, Z. Shirani-Sarmazeh, M. Hosseini-Kharat, J. Lipkowski and M. Saeidifar, *J. Photochem. and Photobiol*., 2015, **144,** 11-19.

24 K. Misra, G. Kr Ghosh, I. Mitra, S. Mukherjee, V. P. Reddy, W. Linert, B. Misini, J. C. Bose, S. Mukhopadhyay and S. Ch Moi, *RSC Adv*., 2015, **5**, 12454-12462.

25 T. M. Sielecki, J. F. Boylan, P. A. Benfield and G. L. Trainor, *J. Med. Chem*., 1999, **43**,1-18.

26 T. Kosta, T. Maryama and M. Otagiri, *Pharm. Res*., 1997, **14**, 1607–1612.

27 A. I. Vogel, *Text Book of Practical Organic Chemistry*, Longman, London, 5th edn., 1989.

28 Z. C. Liu, B. D. Wang, Z. Y. Yang, Y. Li, D. D. Qin and T. R. Li, *Eur. J. Med. Chem*., 2009, **44**, 4477-4484.

29 J. L. Burmeester and F. Basolo, *Inorg. Chem*., 1964, **3**, 1587-1593.

30 Siemens, SMART, SAINT *Area detector control and Integration software*, Siemens Analytical X-ray Instruments Inc., Madison, WI, USA (1996).

31 G. M. Sheldrick, SADABS, *Program for empirical absorption correction of area detector data*, University of Gottingen, Germany (1997).

32 G. M. Sheldrick, SHELXS-97, Program for the solution of crystal structures, University of Gottingen, Gottingen, Germany (1997).

33 G. M. Sheldrick, *Acta Cryst*., 1900, **46**, 467-473.

34 J. Marmur, *J. Mol. Bio*., 1961, **3**, 208-218.

35 M. E. Reichmann, S. A. Rice, C. A. Thomas and P. J. Doty, *J. Am. Chem. Soc*., 1954, **76**, 3047-3053.

36 M. Lee, A.L. Rhodes, M.D. Wyatt, S. Forrow and J.A. Hartley, *Biochemistry*, 1993, **32**, 4237-4245.

37 F. Dimiza, S. Fountoulaki, A. N. Papadopoulos, C.A. Kontogiorgis, V. Tangoulis, C. P. Raptopoulou, V. Psycharis, A. Terzis, D. P. Kessissoglou and G. Psomas, *Dalton Trans*., 2011, **40**, 8555-8568.

38 M. S. Blois, *Nature*, 181 (1958) 1199-1200.

39 T. Nash, *J. Biochem*., 55 (1953) 416-421.

40 L. C. Green, D. A. Wagner, J. Glogowski, P. L. Skipper, J. S. Wishnok and S. R. Tannenbaum, *Anal. Biochem*., 1982, **126**, 131-138.

41 T. Mossman, *J. Immunol. Methods*, 1983, 65 55-63.

42 E.W. Ainscough, A.M. Brodie, A.J. Dobbs, J.D. Ranford and J.M. Waters, *Inorg. Chim. Act*. 1998, **267**, 27-38.

43 F. Basuli, M. Ruf, C. G. Pierpont and S. Bhattacharya, *Inorg. Chem*., 1998, **37**, 6113-6116.

44 D. X. West, I. S. Billeh, J. P. Jasinski, J. M. Jasinski and R. J. Butcher, *Transition Met. Chem*., 1998, **23**, 209-214.

45 A. R. B. Rao and S. Pal, *J. Organomet. Chem*., 2013, **731**, 67-72.

46 Y. P. Tiam, C. Y. Duan, Z. L. Lu and X. Z. You, *Polyhedron*, 1996, **15**, 2263-2271.

47 P. Krishnamoorthy, P. Sathyadevi, R. R. Butorac, A. H. Cowley, N. S. P. Bhuvanesh and N. Dharmaraj, *Dalton Trans*., 2012, **41**, 6842-6854.

48 R. Prabhakaran, R. Sivasamy, J. Angayarkanni, R. Huang, P. Kalaivani, R. Karvembu, F. Dallemer and K. Natarajan, *Inorg. Chim. Act.*, 2011, **374**, 647-653.

49 A. Vignesh, K. Werner and N. Dharmaraj, *RSC Adv*., 2015, **5**, 77948-77957.

50 S. T. Chew, K. M. Lo, S. K. Sinniah, K. S. Sim and K. W. Tan, *RSC Adv*., 2014, **4**, 61232-61247.

51 K. Sampath, S. Sathiyaraj and C. Jayabalakrishnan, *Spectrochim. Acta*, 2013, **115**, 287-296

52 P. Kalaivani, R. Prabhakaran, F. Dallemer, P. Poornima, E. Vaishnavi, E. Ramachandran, V. Vijaya Padma, R. Renganathan and K. Natarajan, *Metallomics*, 2012, **4**, 101-113.

53 T. S. Lobana, G. Bava, A. Castineiras, and R. J. Butcher, *Inorg. Chem. Commun*., 2007, **10**, 506-509.

54 Z. C. Liu, B. D. Wang, Z.Y. Yang, Y. Li, D. D. Qin and T. R. Li, *Eur. J. Med. Chem*. 2009, **44**, 4477-4484.

55 Z.C. Liu, B. D. Wang, B. Li, Q. Wang, Z. Y. Yang, T. R. Li and Y. Li, *Eur. J. Med.Chem.,* 2010, **45**, 5353-5361.

56 W. J. Mei, J. Liu, K. C. Zheng, L. J. Lin, H. Chao, A. X. Li, F. C. Yun and L. N. Ji, *Dalton Trans*., 2003, 1352-1359

57 H.M. Torshizi, R. Mital, T.S. Srivastava, H. Parekh, M.P. Chitnis, *J. Inorg. Biochem.* 1991, **44**, 239-247.

58 M. Tabatabaee, M. Bordbar, M. Ghassemzadeh, M. Tahriri, M. Tahrir, Z. M. Lighvan and B. Neumuller, *Eur. J. Med. Chem*., 2013, **70**, 364-371.

59 M. T. Carter, M. Rodriguez and A. J. Bard, *J. Am. Chem. Soc*., 1989, **111**, 8901-8911.

60 E. S. Koumousi, M. Zampakou, C. P. Raptopoulou, V. Psycharis, C. M. Beavers, S. J. Teat, G. Psomas and T. C. Stamatatos, *Inorg. Chem*. 2012, **51**, 7699-7710.

61 C. Tan, J. Liu, H. Li, W. Zheng, S. Shi, L. Chen and L. Ji, *J. Inorg. Biochem*., 2008, **102**, 347-358.

62 P. Krishnamoorthy, P. Sathyadevi, A. H. Cowley, R. R. Butorac and N. Dharmaraj, Eur. J. Med. Chem., 2011, **46**, 3376-3387.

63 Q. Wang, L. Lu, C. Yuan, K. Pei, Z. Liu, M. Guo and M. Zhu, Chem. Commun., 2010, **46**, 3547-3549.

64 D. Senthil Raja, N. S. P. Bhuvanesh, K. Natarajan, *Eur. J. Med. Chem*., 2011, **46**, 4584-4594.

65 F. A. Beckford, M. Shaloski, G. Leblanc, J. Thessing, L. C. L. Alleyne, A. A. Holder, L. Li and N. P. Seeram, *Dalton Trans*., 2009, **48**, 10757-10764.

66 K. Sampath, S. Sathiyaraj and C. Jayabalakrishnan, *Spectrochim. Act*., 2013, **115**, 287-296.

67 T. Sathiya Kamatchi, P. Kalaivani, P. Poornima, V. Vijaya Padma, F. R. Fronczek and K. Natarajan, *RSC Adv*.,2014,4, 2004

68 M. Mohanraj, G. Ayyannan, G. Raja and C. Jayabalakrishnan, *J. Photochem. Photobiol*., 2016, **158**,164-173.

69 M. Frik, J. Jimenez, V. Vasilevski, M. Carreira, A. D. Almeida, E. Gascon, F. Benoit, M. Sanau, A. Casini and M. Contel, *Inorg. Chem. Front*., 2014, **1**, 231-241.

70 E. Sindhuja, R. Ramesh, N. Dharmaraj and Y. Liu, *Inorg. Chim. Acta*, 2014, **416**, 1-12.

Compound	**1**	**2**	**3**

Table 1.

Empirical formula	$C_{14}H_{11}BrN_2O_3$	$C_{32}H_{24}BrN_2O_3PPd$	$C_{32}H_{24}BrN_2O_3AsPd$
CCDC	1482486	1482487	1482488
Formula weight	335.16	701.81	745.76
Temperature	296(2) K	296(2) K	296(2) K
Wavelength	0.71073Å	0.71073 Å	0.71073Å
Crystal system	Orthorhombic	Monoclinic	Monoclinic
Space group	$Pna2_1$	$P\ 2_1/c$	$P2_1/c$
Unit cell dimensions			
a (Å)	8.0392(7)	15.3568(5)	15.7334(6)
b (Å)	25.680(3)	9.0646(2)	9.1057(2)
c (Å)	6.2125(5)	21.4790(6)	21.2449(7)
α (°)	90	90	90
β (°)	90	108.729(10)	109.0330(10)
γ (°)	90	90	90
Volume ($Å^3$)	1282.5(2)	2831.62(14)	2877.23(16)
Z	4	4	4
Density (calculated) Mg/m^3	1.736	1.646	1.722
Absorption coefficient mm^{-1}	3.214	2.160	3.211
F(000)	672	1400	1472
Crystal size/mm^3	0.35 x 0.30 x 0.30	0.30 x 0.25 x 0.20	0.35 x 0.30 x 0.30
Theta range for data collection (°)	1.59 to 28.28	1.40 to 28.34	1.37 to 28.32
Index ranges	-10 <= h <= 10, -21 <= k <= 34, -8 <= l <= 7	-18 <= h <= 20, -11 <= k <= 12, -28 <= l <= 28	-20 <= h<= 19, -12 <=k <= 12, -26 <= l <= 28
Reflections collected	7340	21142	21646
Independent reflections	3099 [R(int) = 0.0265]	6978 [R(int) = 0.0266]	7151 [R(int) = 0.0287]
Refinement method	Full-matrix least-squares on F^2	Full-matrix least-squares on F^2	Full-matrix least-squares on F^2
Data/restraints/parameters	3099/1/181	6978/0/361	7151/0/361
Goodness-of-fit on F^2	1.018	1.118	1.114
Final R indices [$I > 2\sigma(I)$]	R_1 = 0.0297, wR_2 = 0.0699	R_1 = 0.0302, wR_2 = 0.0759	R_1 = 0.0353, wR_2 = 0.0846
R indices (all data)	R_1 = 0.0398, wR_2 = 0.0760	R_1 = 0.0513, wR_2 = 0.0996	R_1 = 0.0623, wR_2 = 0.1098
Largest diff. peak and hole e.$Å^{-3}$	0.274and -0.329	0.690 and -0.864	0.740 and -0.851

Crystal and structure refinement data.

Table 2. Selected bond lengths [Å] and bond angles [°] for ligand **1.**

Bond lengths	**1**

N(2)-C(8)	1.354(4)
C(7) N(1)	1.278(4)
N(1) N(2)	1.378(3)
C(8) O(2)	1.229(3)
C(8)-N(2)	1.354(4)
C(1) O(1)	1.356(3)
C(12)-O(3)	1.356(3)
Bond angles	
O(1)-C(1)-C(6)	122.7(3)
C(7)-N(1)-N(2)	116.1(2)
O(2)-C(8)-N(2)	122.4(3)
N(1)-C(7)-C(6)	121.8(3)
N(2)-C(8)-C(9)	115.5(2)

Table 3. Selected bond lengths [Å] and angles [°] of palladium(II) complexes **2** and **3**.

Bond lengths	**2**		**3**
Pd(1)-N(1)	1.981(2)	Pd(1)-N(1)	1.970(3)
Pd(1)-O(1)	1.9961(19)	Pd(1)-O(1)	1.993(2)
Pd(1)-O(3)	1.9625(19)	Pd(1)-O(3)	1.958(2)
Pd(1)-P(1)	2.2864(8)	Pd(1)-As(1)	2.392(5)
O(1)-C(1)	1.308(3)	O(1)-C(7)	1.303(4)
C(8)-N(1)	1.285(3)	C(8)-N(1)	1.284(4)
Bond angles			
N(2)-N(1)-Pd(1)	114.45(17)	N(2)-N(1)-Pd(1)	114.5(2)
O(3)-Pd(1)-N(1)	94.35(9)	O(3)-Pd(1)-N(1)	95.02(11)
N(1)-Pd(1)-P(1)	171.44(6)	N(1)-Pd(1)-As(1)	171.14(8)
O(3)-Pd(1)-O(1)	172.74(8)	O(3)-Pd(1)-O(1)	172.74(8)
O(3)-Pd(1)-P(1)	90.17(6)	O(3)-Pd(1)-As(1)	89.34(8)

Table 4. DNA binding constant (K_b), quenching constant (K_q) and apparent binding constant (K_{app}) values

Compounds	K_b (M^{-1})	K_q (M^{-1})	K_{app} (M^{-1})
1	9.96×10^3	2.54×10^4	1.8×10^5
2	6.78×10^4	3.66×10^4	2.7×10^5
3	2.04×10^4	3.01×10^4	2.2×10^5

Table 5. Quenching constant (K_q), binding constant (K_{bin}), and number of binding sites (n) for the interactions of compounds (**1-3**) with BSA

Compounds	K_q (M^{-1})	K_{bin} (M^{-1})	*n*
1	3.4×10^4	9.0×10^4	0.95
2	9.4×10^4	2.3×10^5	1.42
3	5.2×10^4	1.0×10^5	1.15

Table.6. Antioxidant activity of the ligand and new palladium(II) complexes with standard ascorbic acid.

Compounds	IC_{50} values (μM)		
	$DPPH^{\cdot}$	$OH^{\cdot}$	$NO^{\cdot}$
1	98.73 ± 1.2	43.97 ± 1.4	84.72 ± 0.7
2	42.84 ± 0.9	14.06 ± 1.2	53.64 ± 2.5
3	48.63 ± 1.4	19.74 ± 1.8	62.16 ± 2.8
Ascorbic acid (Asc)	27.71 ± 0.7	5.12 ± 0.2	37.52 ± 0.5

Table 7. Cytotoxic activity of the ligand and palladium(II) complexes against the HeLa and MCF-7 cancer cell lines.

Compounds	IC_{50} values (μM)	
	HeLa	MCF-7
1	96.76 ± 2.3	99.23 ± 2.8
2	31.64 ± 1.2	30.32 ± 0.8
3	44.62 ± 1.1	40.13 ± 0.6
Cisplatin	16.21 ± 0.9	15.35 ± 1

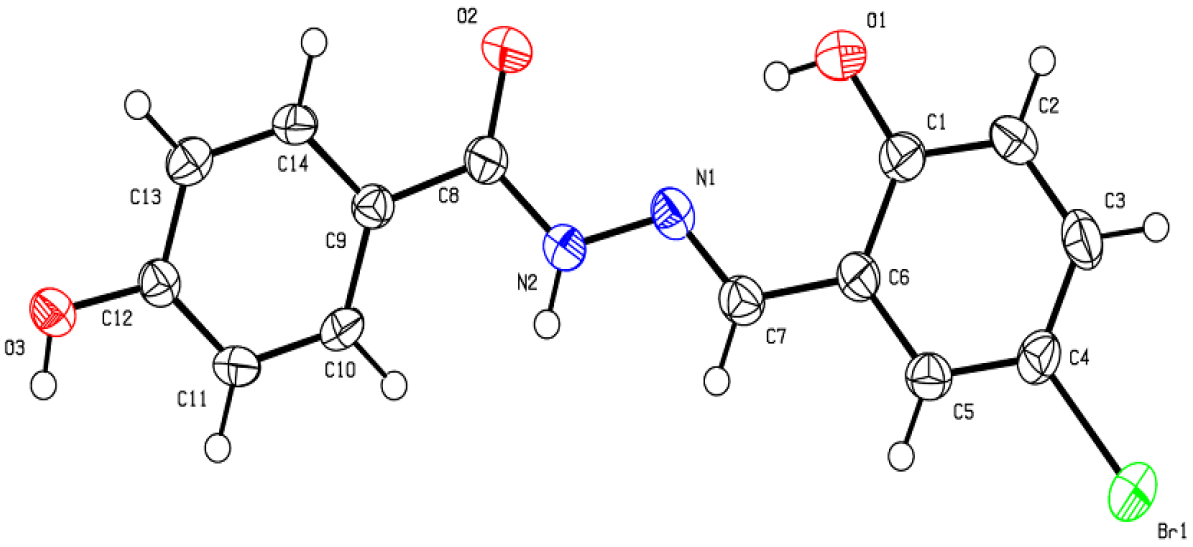

Figure 1. ORTEP diagram of **1** with thermal ellipsoid at 50% probability

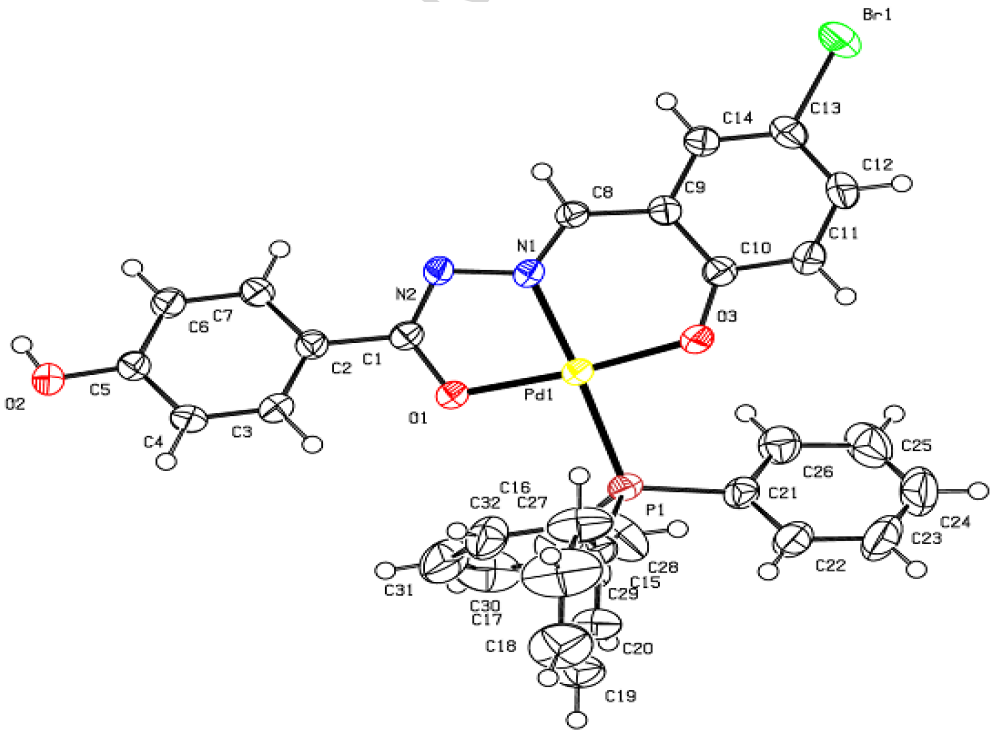

Figure 2. ORTEP diagram of **2** with thermal ellipsoid at 50% probability

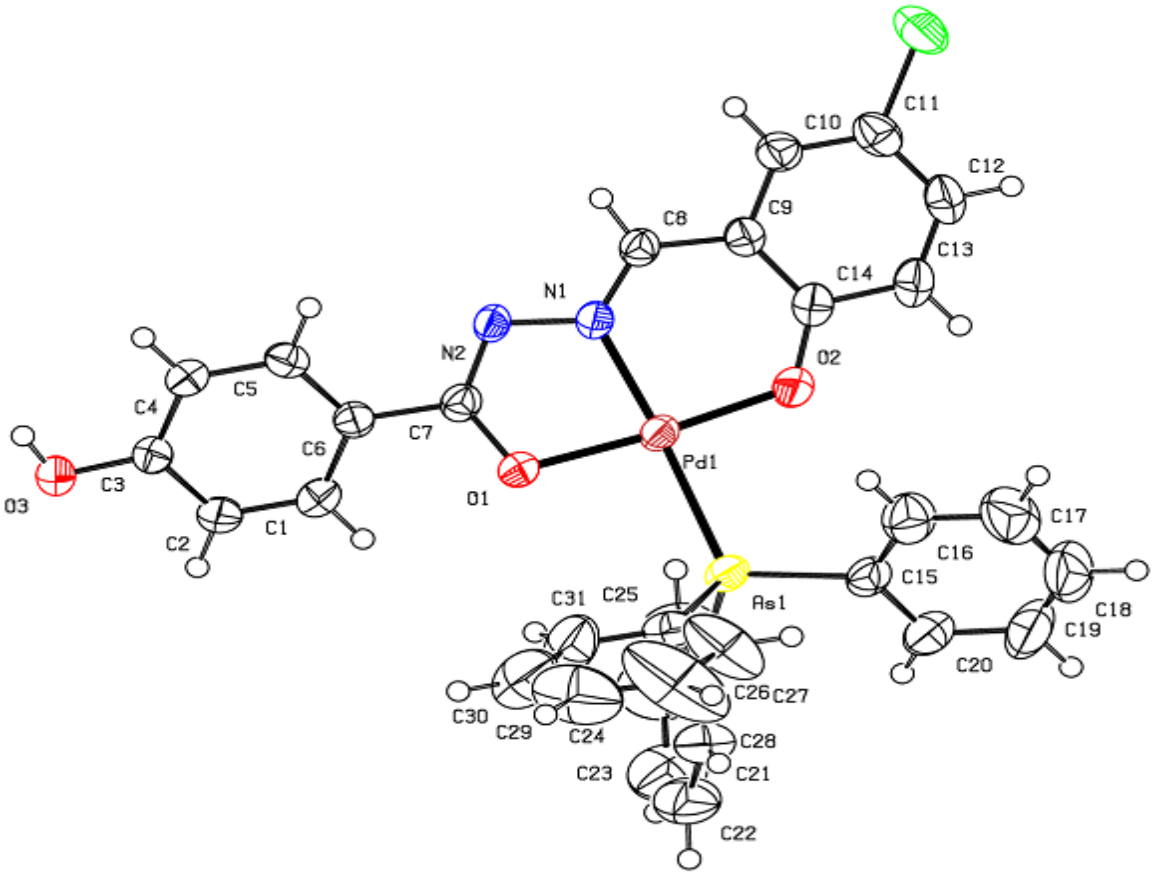

Figure 3. ORTEP diagram of **3** with thermal ellipsoid at 50% probability

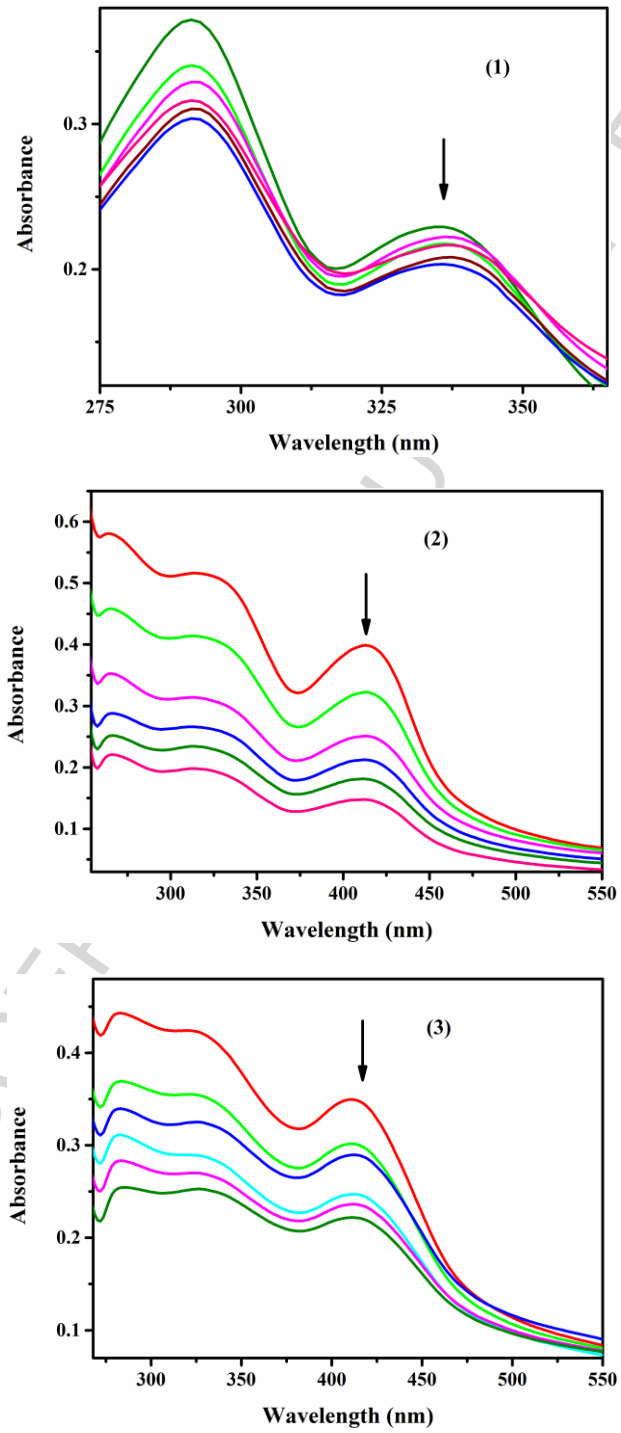

Figure 4. Electronic spectra of the compounds (**1**), (**2**) and (**3**) in Tris-HCl buffer upon addition of CT-DNA. [Compound] = 25µM, [DNA] = 0-50µM. Arrow shows that the absorption intensities decrease upon increasing DNA concentration

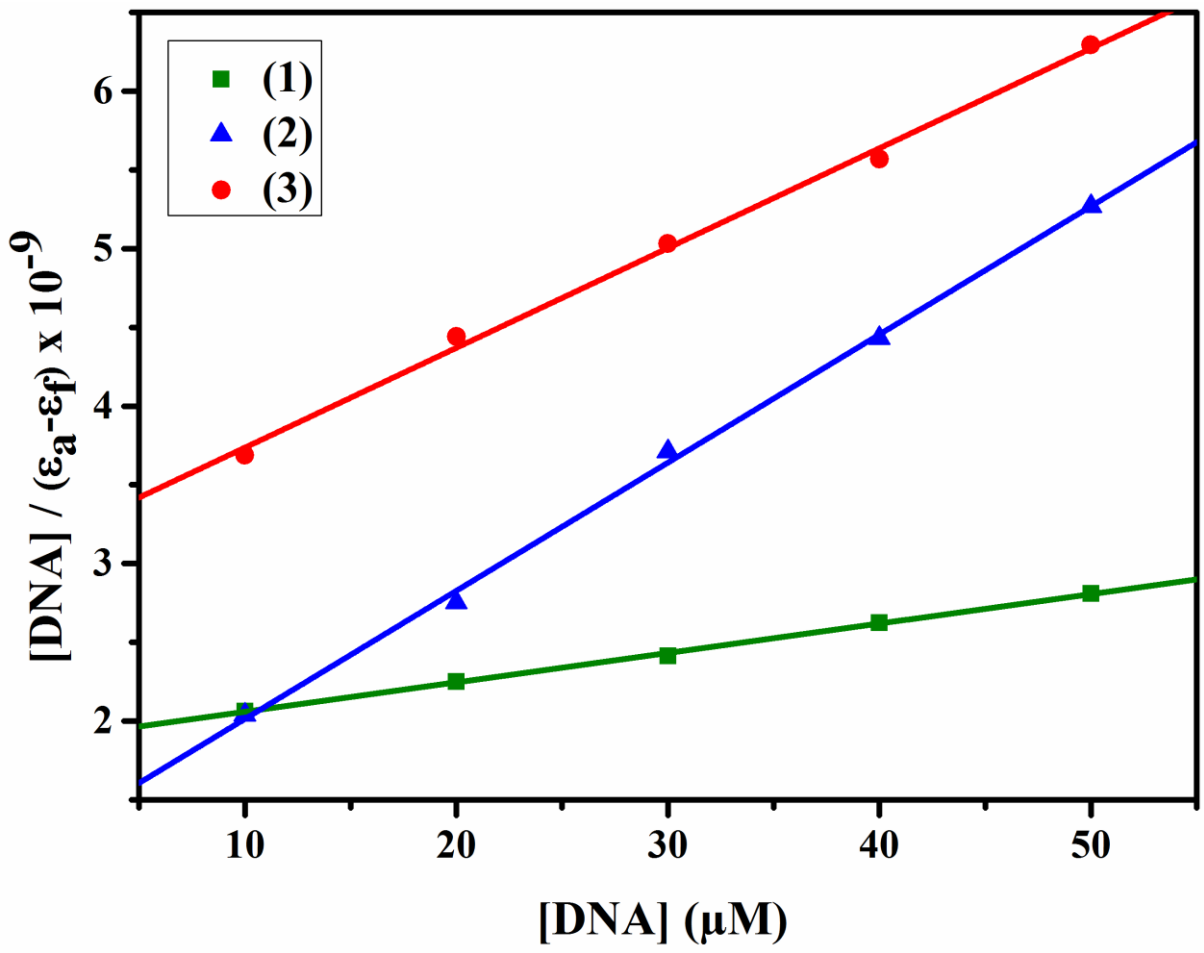

Figure 5. Plots of [DNA]/(ε_a-ε_f) versus [DNA] for compounds **1-3** with CT-DNA.

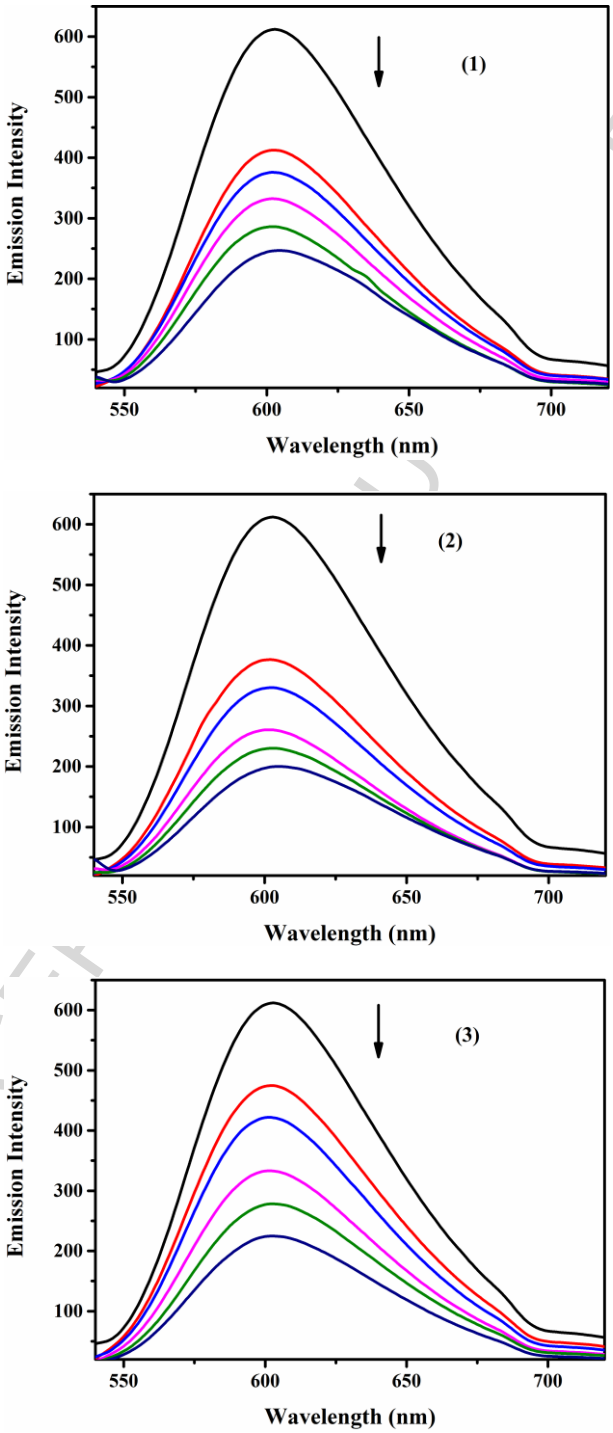

Figure 6. Fluorescence quenching curves of ethidium bromide bound to DNA: **1**, **2** and **3**. [DNA] = 10 μM, [EB] = 10 μM, and [complex] = 0-50 μM. Arrow shows the emission intensity changes upon increasing complex concentration.

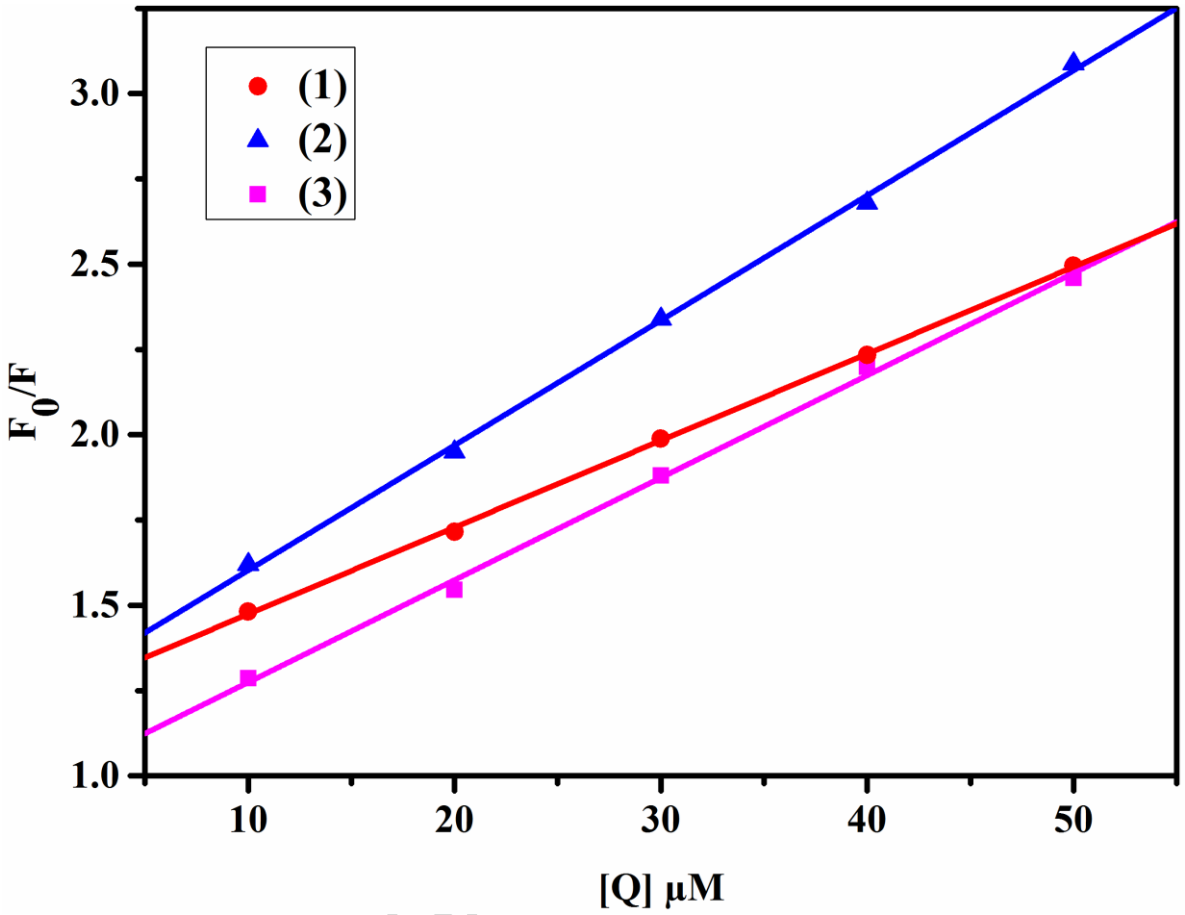

Figure 7. Stern-Volmer plots of the EB-DNA fluorescence titration for compound **1-3**.

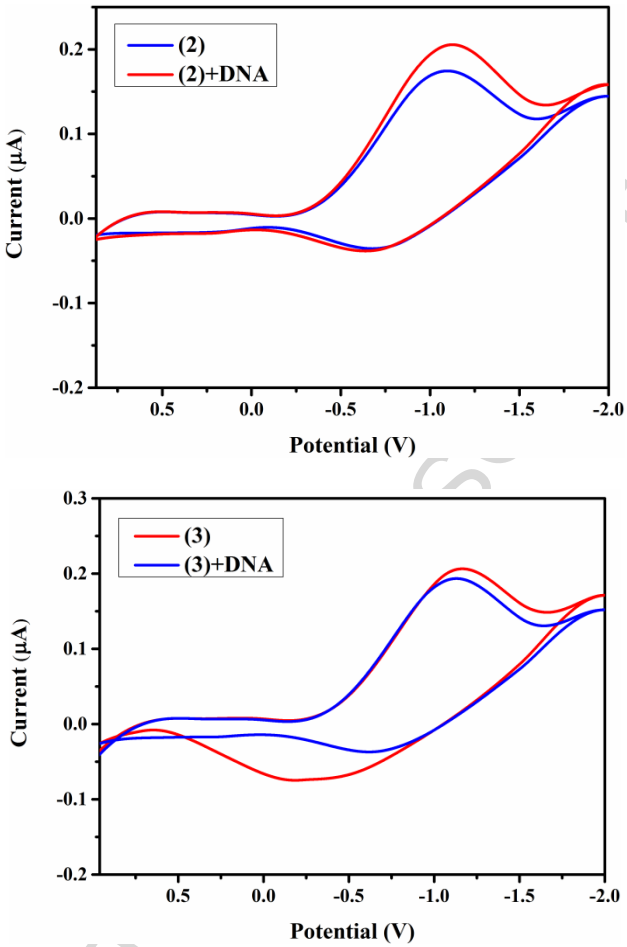

Figure 8. Cyclic voltammogram of complex **2** and **3** in the absence and presence (inner line) of DNA (10 μM). Scan rate: 100 mV s^{-1}

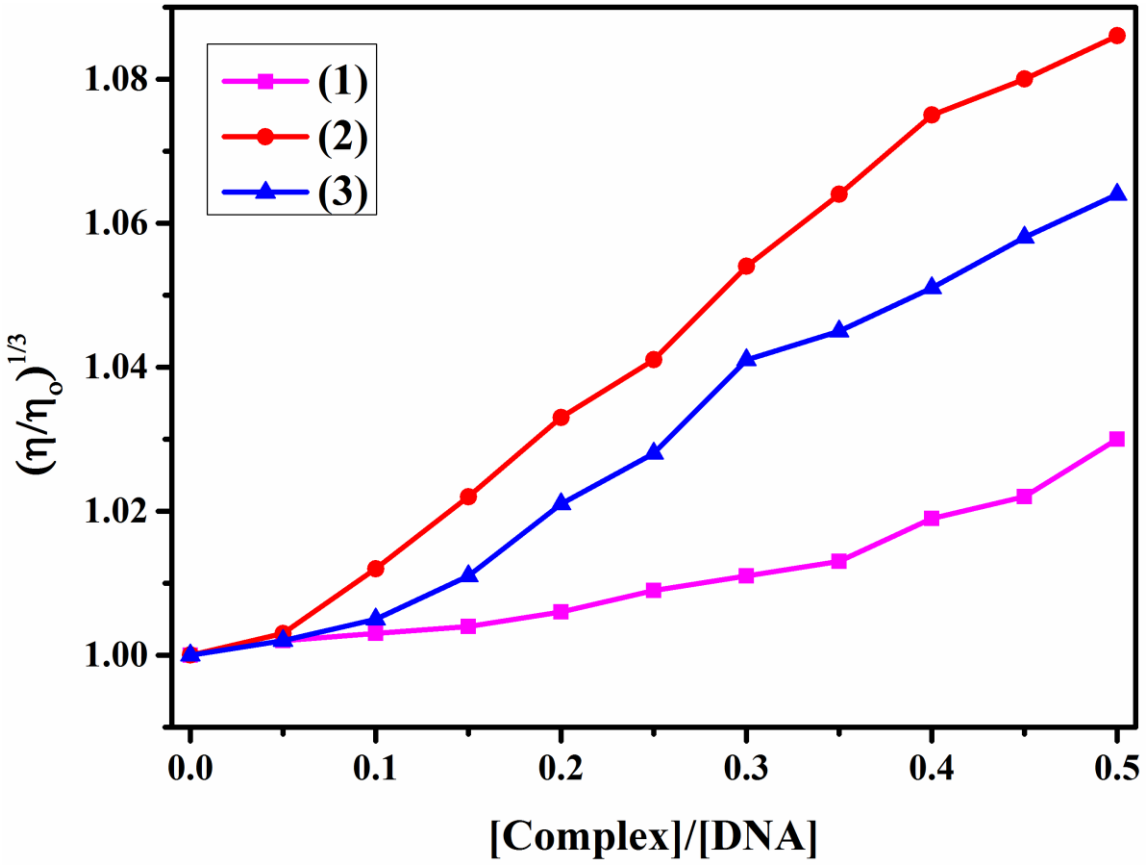

Figure 9. Effect of the compounds (**1-3**) on the viscosity of CT-DNA.

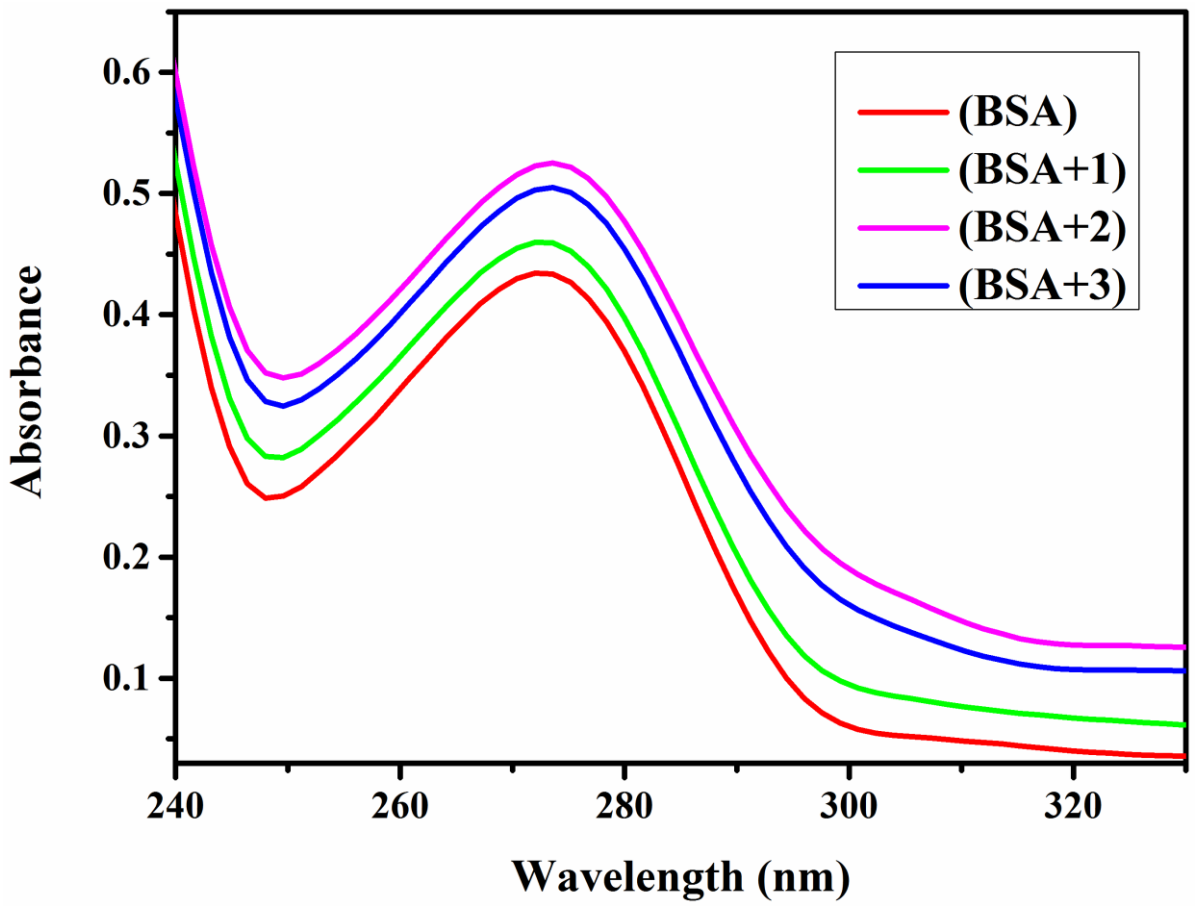

Figure 10. Absorbance titrations of **1-3** with BSA.

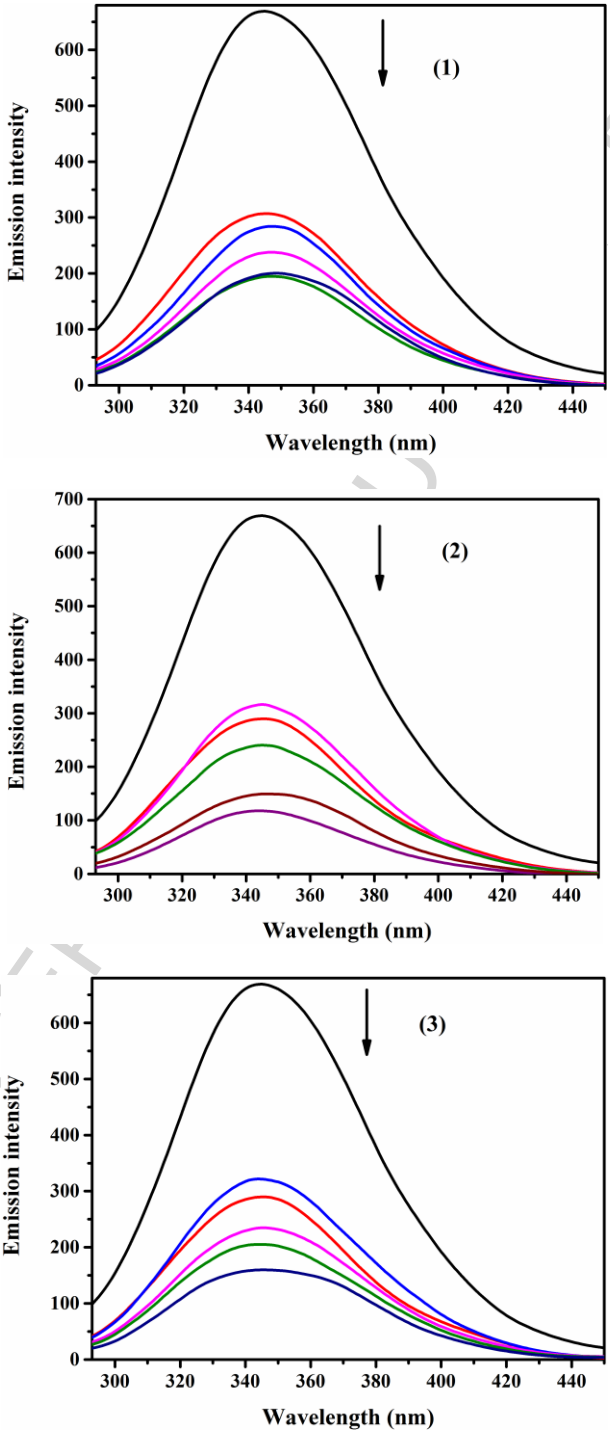

Figure 11. Fluorescence titrations of **1-3** (0-25μM) with BSA (1μM).

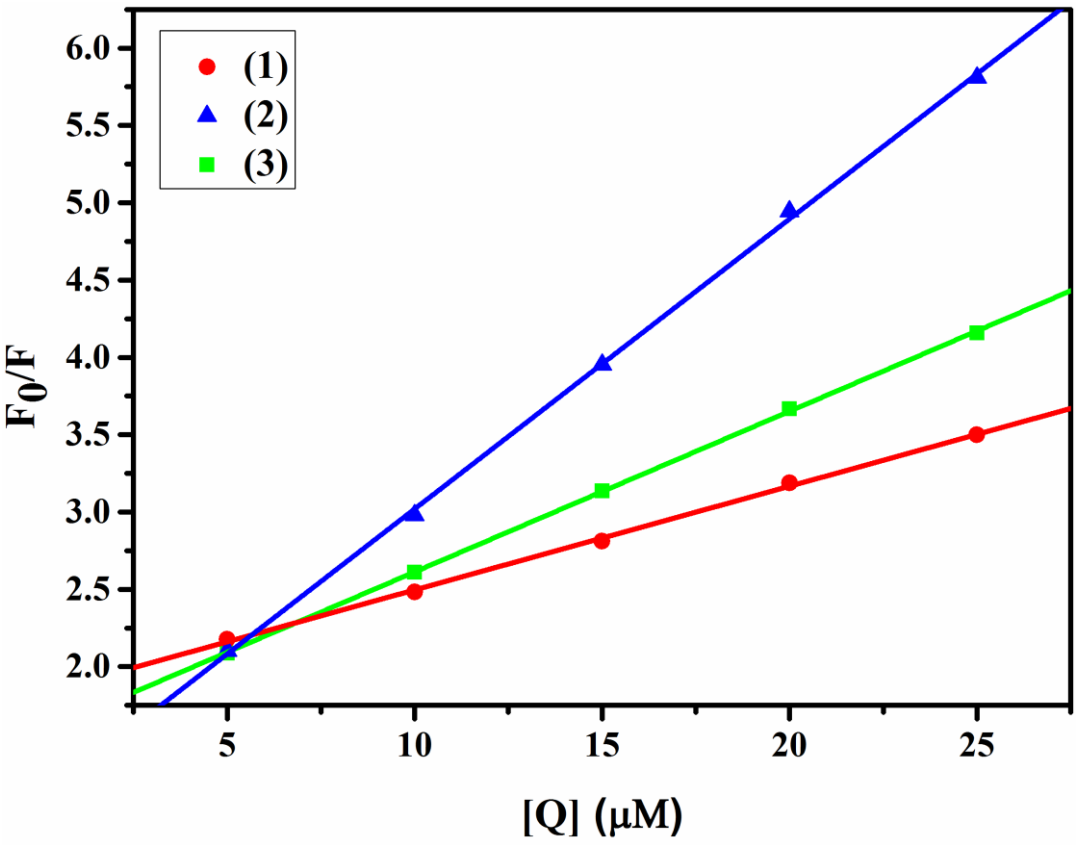

Figure 12. Stern-Volmer plots of the fluorescence titrations of **1-3** with BSA

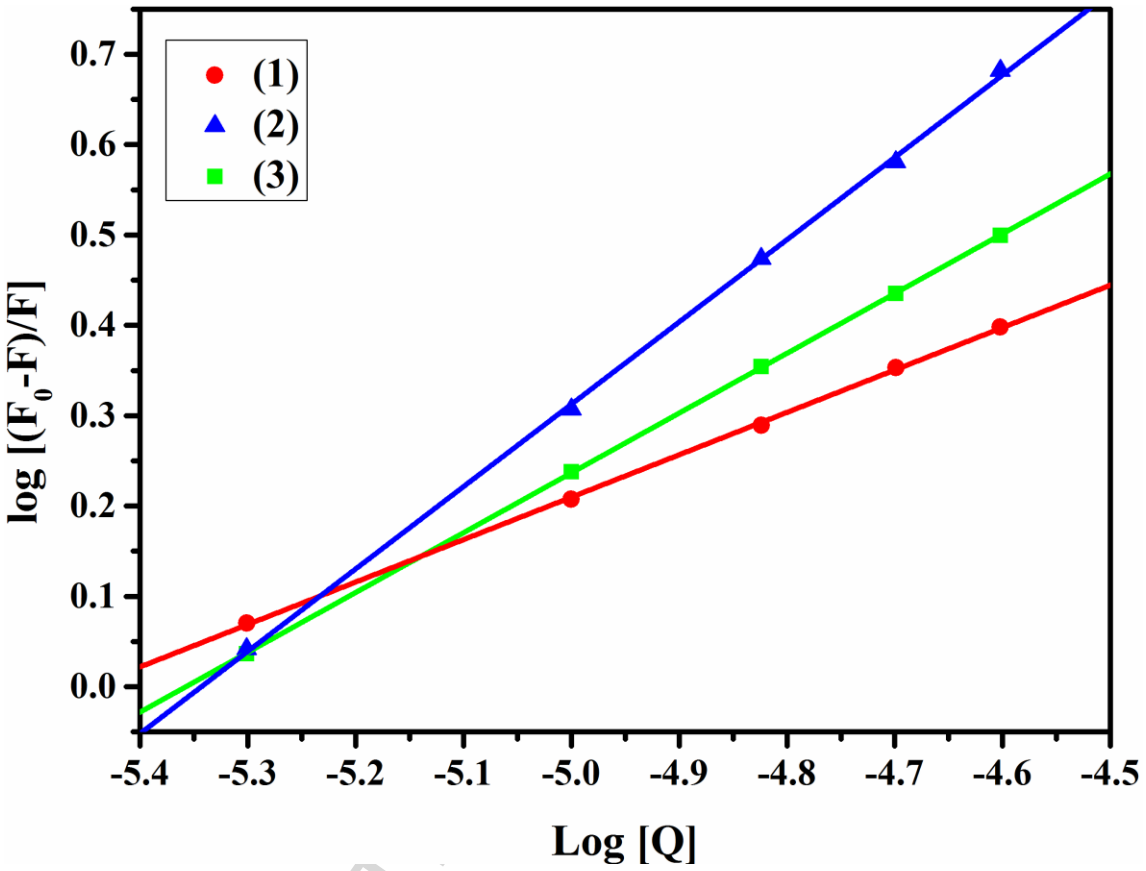

Figure 13. Plot of log[Q] versus log[(F_0-F)/F]

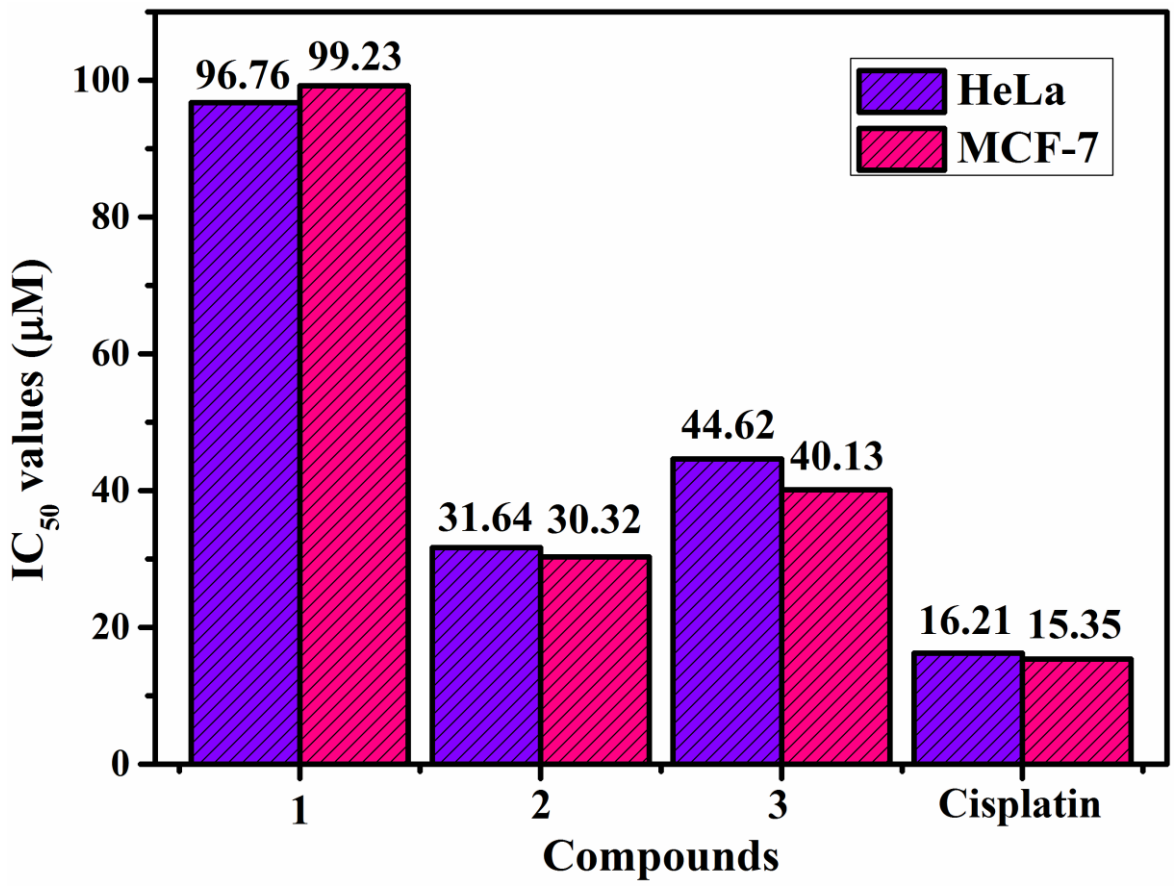

Figure. 14. Cytotoxic activity of compounds, **1-3** with standard, cisplatin.

Graphical Abstract

New palladium(II) hydrazone complexes: Synthesis, structure and biological evaluation

Ganesan Ayyannan[a], Maruthachalam Mohanraj[a], Gunasekaran Raja[a], Nanjan Bhuvanesh[b], Raju Nandhakumar[b], Chinnasamy Jayabalakrishnan[a]*

[a]*Post-Graduate and Research Department of Chemistry, Sri Ramakrishna Mission Vidyalaya College of Arts and Science, Coimbatore - 641 020, Tamil Nadu, India.*

[b]*Department of Chemistry, Karunya University, Karunya nagar, Coimbatore - 641 114, Tamil Nadu, India.*

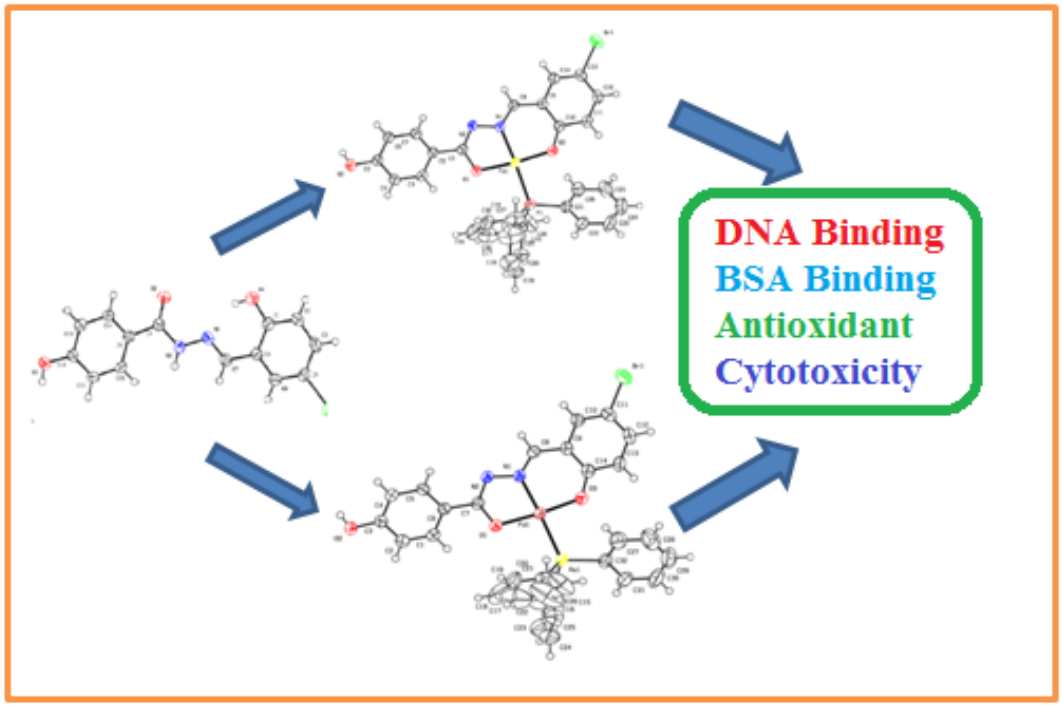

Highlights

- Molecular structure of ligand and complexes was elucidated by X-ray diffraction study
- Interaction of CT-DNA with small molecules *via* intercalatively
- Protein interact with complexes more strongly than ligand
- The complexes possess significant antioxidative property against DPPH radical
- The complex **2** shows higher IC_{50} value than the other complex against tumor cells